scientific reports

Check for updates

OPEN

Theoretical background of the operating parameters of the satellite working mechanism of the hydraulic positive displacement machine

Pawel Sliwinski

This article describes a method for determining the instantaneous geometric working volume of a satellite mechanism that is commonly used as a working mechanism in positive displacement machines (pump and motor). A new mathematical formula for calculating the instantaneous geometric working volume as a function of the angle of rotation of the shaft (rotor) has been proposed. For the satellite mechanism operating as a pump, the mathematical formula for the instantaneous flow rate in this mechanism as a function of the angle of rotation of the rotor (shaft) has been developed. The mathematical formula for the torque indicated in this mechanism (pumping operation) was also developed. Similarly, analyses were carried out for a satellite mechanism operating as a motor. Mathematical formulae were presented to calculate the instantaneous speed of the motor shaft and the instantaneous pressure in the motor's supply port. To confirm the results of the mathematical analyses, experimental tests were carried out with a prototype satellite machine at a low constant speed. The satellite machine was tested in both pump and motor mode. The results of the tests confirmed that the torque on the shaft is not constant in both pump and motor operation at a constant pressure drop in this machine. This torque depends strictly on the instantaneous working volume of the machine and is therefore a function of the angle of rotation of the shaft. Similarly, at a constant speed, the flow rate (motor absorption) in the machine is also not constant.

Keywords Non-circular mechanism, Satellite mechanism, Pump, Motor, Satellite, Rotor, Curvature, Working volume

The positive displacement pump and the hydraulic motor (rotary or linear) are the basic and most important components in a hydrostatic drive system. The pump is the source of the fluid flow in the hydraulic system. The hydraulic motor, on the other hand, is the executing element in this system. In recent years, satellite displacement machines, especially satellite motors, have attracted increasing interest from researchers around the world. The first satellite motor was developed and patented by Eng. B. Sieniawski in 1974[1]. It was a motor with a 3×4 type satellite mechanism (three-humped rotor and four-humped curvature – Fig. 1)[2–6]. This motor is still in production[7].

The design methodology of this motor is described in[8]. Nowadays, the next generation of satellite motors, i.e. motors with a 4×6 type mechanism (Fig. 1), are also being manufactured[9–11]. The first satellite mechanism of the 4×6 type was also developed and put into production by Eng. B. Sieniawski in 1981[12]. Another type of satellite mechanism was the 6×8 type, which was also developed and put into production by Eng. B. Sieniawski in 1997 (Fig. 1)[13,14]. Satellite motors are characterised by a high torque-to-mass ratio of the mechanism and the ability to work with low-viscosity fluids (especially oil-in-water emulsions of the HFA-E type and water). They are therefore widely used to drive a variety of machines and equipment, especially machinery and hand tools in the mining industry.

New types of satellite mechanisms are still being developed, with a different number of humps on the rotor and the curvature. In publications[16–19], for example, satellite mechanisms of types 1×1, 2×2, 2×3, 2×4, and 3×3 were presented. However, the design methodology of these mechanisms was briefly characterised in

Faculty of Mechanical Engineering and Ship Technology, Gdansk University of Technology, 11/12 G. Narutowicz Str, Gdańsk 80-233, Poland. email: pawel.sliwinski@pg.edu.pl

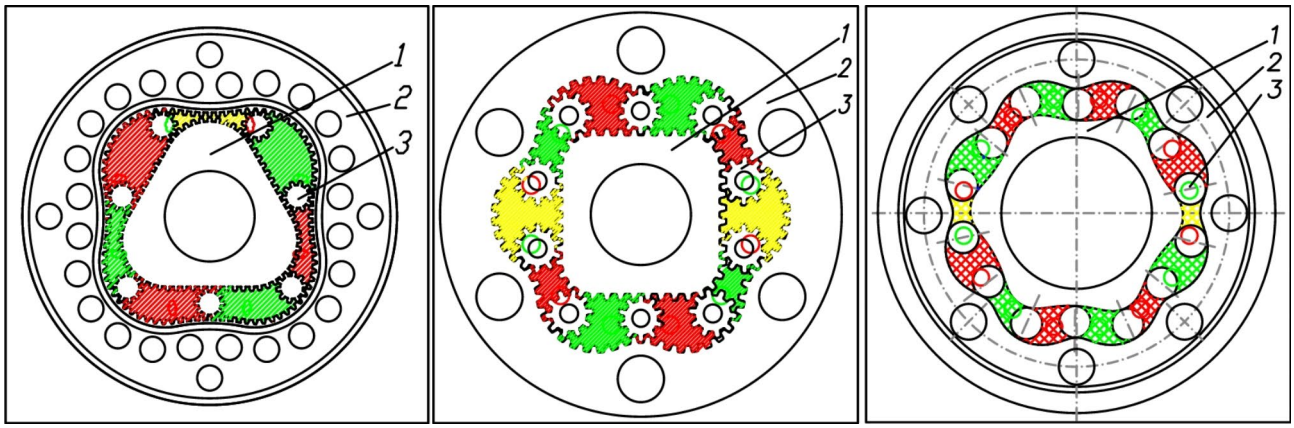

Fig. 1. Satellite mechanisms: type 3 × 4 (left), type 4 × 6 9 (middle) and type 6 × 8 (right): 1—rotor, 2—curvature, 3—satellite[15].

articles[18,20,21]. The article[22] deals in particular with the selection of the shape of the curvature and the rotor of the 2 × 2 type mechanism. The 1 × 1 type mechanism is a specialty. It is a mechanism consisting of an internally toothed gear (curvature), an externally toothed gear (rotor) eccentric to the axis of the curvature, and two small gears (satellites) that interact with the curvature and the rotor[17]. In the work[23] the mechanical losses and thus the mechanical efficiency of the 2 × 4 mechanism were estimated analytically. Satellite mechanisms of the 1 × 1, 2 × 2, 2 × 3, 2 × 4, and 3 × 3 types have not found practical application so far. The mechanisms shown in Fig. 1, i.e. the 3 × 4, 4 × 6, and 6 × 8 type mechanisms have found practical application. In the work[5] a method of manufacturing a 3 × 4 mechanism was presented (the WEDM method).

However, the 4 × 6 satellite mechanisms are currently the most popular. Newer and newer designs of these mechanisms are being developed. In publications[15,18,24–26] methods for designing satellite mechanisms with a sinusoidal rotor outline are presented. However, the article[27] presents a method for designing a mechanism in which the rotor and the curvature consist of arcs (non-circular double-arc gear). The construction of the 4 × 6 type mechanism is also described in[28].

The 4 × 5 type satellite mechanism is also known, although it is not as popular as the 4 × 6 mechanism. It has been used as a working mechanism in the hydraulic motor[29,30] and in the pressure intensifier[31].

The 6 × 8 type satellite mechanism can be indicated as a new trend in the development of satellite mechanisms. The first work on a hydraulic motor using this mechanism was published in 2003[14]. The next significant works on this mechanism were published in 2022[15] and 2024[32] and mainly concern the methods of its design.

The features of the satellite mechanisms that affect their main operating parameters are also described. Publication[33], for example, describes a method for determining the theoretical working volume of satellite mechanisms of different types. But in[34] a method for determining the geometrical working volume of these mechanisms is described. However, publications[32,35] describe guidelines for the design of commutation unit in satellite machines and in publication[36] the methods to expand feed channels in satellite machines.

Satellite mechanisms are not only used in hydraulic motors. D. Sieniawski made the first attempt to use a 3 × 4 type mechanism in a satellite pump[37]. The pump with this mechanism was not put into production. In recent years, on the other hand, the first pumps fitted with a satellite working mechanism of the 4 × 6 type have been developed and built. The first information about the satellite pump with the 4 × 6 type satellite mechanism was given in[21,38,39]. Further work on the development of the satellite pump design was described by L. Osiecki in[40,41]. The latest design solution of the satellite pump can be found in the patent description in[42].

Researchers are not only interested in developing the design of satellite machines but also in analysing the physical phenomena that occur in these machines. Papers[27,43] have characterised the forces acting in the interacting teeth of the mechanism. Studies have also been carried out on the influence of liquids other than mineral oil on energy losses in satellite machines. These fluids were water and rapeseed oil. In the publication[44] the influence of motor load and operating time on energy conversion efficiency is presented when this motor was supplied with rapeseed oil. Publications[45,46] described the volumetric losses in satellite motors supplied with water. In[47], on the other hand, the volumetric losses in a satellite pump were described. In addition, the mechanical losses that occur in both the satellite pump[48] and the satellite motor[49] when supplied with both water and mineral oil were analysed and described. In the paper[50] the influence of water and mineral oil on the pressure losses in satellite machines was described. A method for determining these losses was also proposed in these papers. Jasinski, on the other hand, investigated the behaviour of a satellite motor under conditions of so-called thermal shock, i.e. when a very cold motor is fed with a hot working medium[6].

As the shaft rotates, each working chamber changes its volume from a minimum value to a maximum value. This volume changes cyclically[51–54]. The volume of each working chamber of a positive displacement machine can be determined from the design documentation of this machine or by precise measurements of the components of the working mechanism (as described in[34,54]). The filling and emptying of the chambers with working liquid takes place while the machine shaft is rotating. The change in the volume of the working

chambers as the shaft rotates causes the geometric working volume to change from a value of q_{g-min} to q_{g-max}[34]. A change in the geometric working volume is therefore accompanied by:

- in the case of a pump – a non-uniformity (pulsation) of the pump delivery (output flow rate) and a non-uniformity of the torque on the pump shaft;
- in the case of a hydraulic motor – a non-uniformity (pulsation) of the rotational speed of the motor shaft and a non-uniformity (pulsation) of the pressure drop in the motor.

Studies on the change in the geometric working volume as a function of the angle of rotation of the shaft of a satellite displacement machine have not yet been carried out on a large scale. The first attempts at an analysis were undertaken by Kujawski. However, Kujawski's investigations were limited to satellite mechanisms of the 3×4 type[51,55]. Kujawski was the first to attempt to determine the torque based on the dimensions of the geometry of the rotor and the contact points of the satellites with this rotor, i.e. without knowledge of the geometric working volume[55]. Another attempt to determine the torque, similar to Kujawski in[55], was made by Oshima et al. in[29,30] for a 4×5 type satellite mechanism.

Therefore, this paper aims to develop mathematical formulae that allow to calculate for each type of satellite mechanism:

1. the change in the volume of the one working chamber as a function of the angle of rotation of the rotor (shaft);
2. the volumes of the filling chambers and the volumes of the emptying chambers as a function of the angle of rotation of the rotor;
3. the total volume of the satellite mechanism;
4. instantaneous value of the geometric working volume as a function of the angle of rotation of the shaft;
5. for pump operation (at a constant shaft speed and constant pressure increase in the pump):
   - liquid flow rate in the one working chamber as a function of the shaft rotation angle;
   - instantaneous flow rate of the liquid in the satellite mechanism as a function of the shaft rotation angle;
   - the average flow rate in the pump;
   - the torque generated by the one working chamber as a function of the angle of rotation of the shaft based on the rotor geometry;
   - instantaneous torque generated by the entire working mechanism as a function of the shaft rotation angle;
   - irregularity (pulsation) of the pump delivery;
   - irregularity (pulsation) of the torque;
6. for motor operation (at a constant flow rate in the working mechanism and constant load (torque) of the motor):
   - instantaneous rotational speed of the motor shaft for a constant flow rate;
   - average rotational speed of the motor shaft;
   - instantaneous pressure in the supply connection of the motor;
   - the average pressure in the supply connection of the motor;
   - irregularity (pulsation) of the pressure in the motor supply connection;
   - irregularity (pulsation) of the rotational speed of the motor shaft.

To confirm the validity of the above-mentioned mathematical relationships, experimental tests were also carried out on a satellite machine operating as a pump and as a hydraulic motor.

Working mechanism of the satellite positive displacement machine

In satellite positive displacement machines, i.e. pumps and motors, the working mechanism is the satellite mechanism as shown in Fig. 1. The 4×6 satellite mechanism is commonly used in currently developed machine designs. The design of this mechanism is shown in Figs. 2 and 3.

A 4×6 satellite mechanism developed according to the methodology described in[15] was analysed. The radius R of the rotor pitch line of this mechanism is described by the equation[28]:

$$R = \frac{D}{2} - A \cdot \cos(n_R \cdot \alpha) + B \cdot \cos(2 \cdot n_R \cdot \alpha) \tag{1}$$

where n_R is the number of rotor humps (Fig. 4). The other parameters, i.e. α, A, B, D are shown in Fig. 4.

The parameters of the investigated and analysed mechanism are listed in Table 1.

In the table above:

- n_E – the number of curvature humps,
- z_E – the number of teeth on the curvature,
- z_R – the number of teeth on the rotor,
- z_S – the number of teeth on the satellite, m – the module of the teeth,
- H – the height of the mechanism,
- q_g – the geometric working volume,
- β_R – the central angle covering one half of the cycle of the rotor pitch curve (the angle between the axis of symmetry OR of the hump concavity and the axis of symmetry OZ of the hump convexity) (Figs. 3 and 4)[15]:

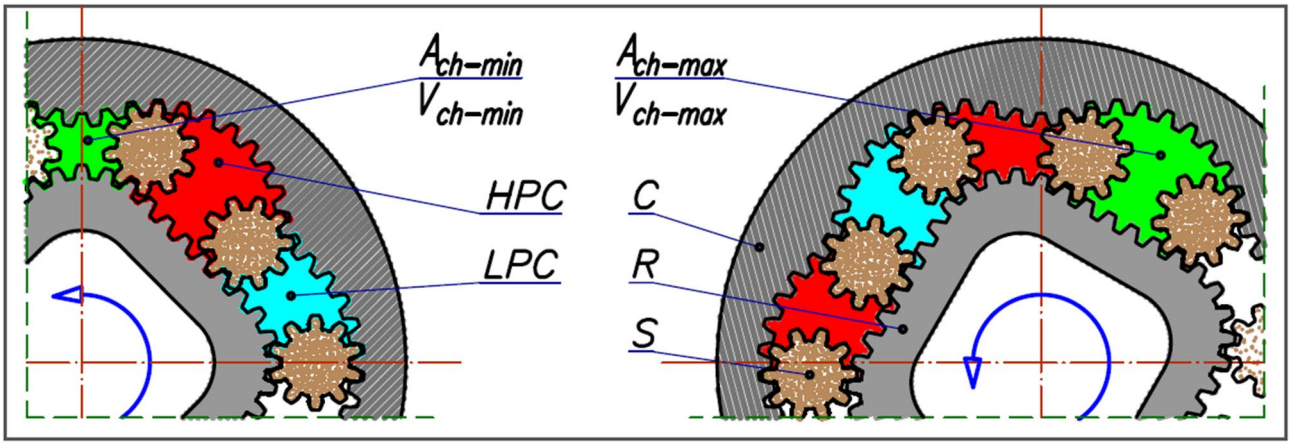

Fig. 2. Satellite mechanism type 4 × 6: C – curvature, R – rotor, S – satellite, HPC – high-pressure working chamber, LPC – low-pressure working chamber, $A_{ch\text{-}min}$ – area of the chamber with minimum volume $V_{ch\text{-}min}$, $A_{ch\text{-}max}$ – area of the chamber with maximum volume $V_{ch\text{-}max}$[34,44].

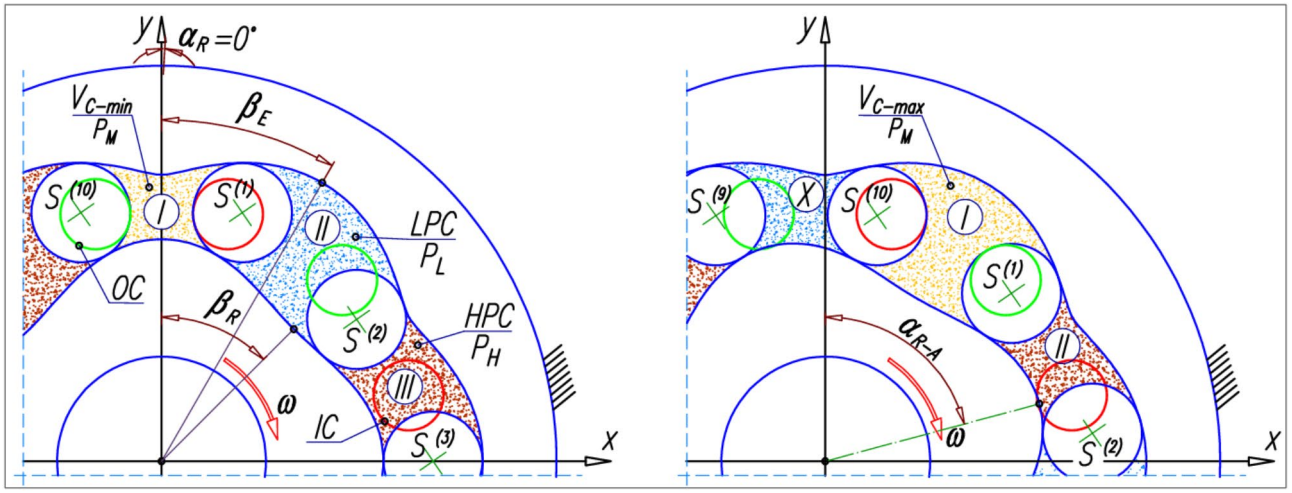

Fig. 3. Satellite mechanism type 4 × 6: β_R and β_E – characteristics angle of the rotor R and curvature (description in the text), $S^{(1)} \div S^{(10)}$ – satellites, IC – inflow channel, OC – outflow channel, p_H – high pressure, p_L – low pressure, p_M – medium pressure, α_R – angle of the rotor (shaft) rotation, $\alpha_{R\text{-}A}$ – angle of rotor rotation for change from V_{min} to V_{max}, ω – angular velocity of the rotor, I ÷ X – working chambers. (created in Autodesk Autocad 2024, https://www.autodesk.com/)

$$\beta_R = \frac{180^o}{n_R} \tag{2}$$

- β_E – the central angle that covering one half of the cycle of the curvature pitch curve (the angle between the axis of symmetry of the hump concavity and the axis of symmetry of the hump convexity) (Fig. 3)[15]:

$$\beta_E = \frac{180^o}{n_E} \tag{3}$$

- $A_{ch\text{-}min}$ – area of the chamber with minimum volume $V_{ch\text{-}min}$ (Figs. 2 and 3),
- $A_{ch\text{-}max}$ – area of the chamber with maximum volume $V_{ch\text{-}max}$ (Figs. 2 and 3).

In a satellite mechanism, the number n_{ch} of working chambers is equal to the number n_S of satellites, that is (Figs. 2 and 3)[15]:

$$n_{ch} = n_S = n_E + n_R \tag{4}$$

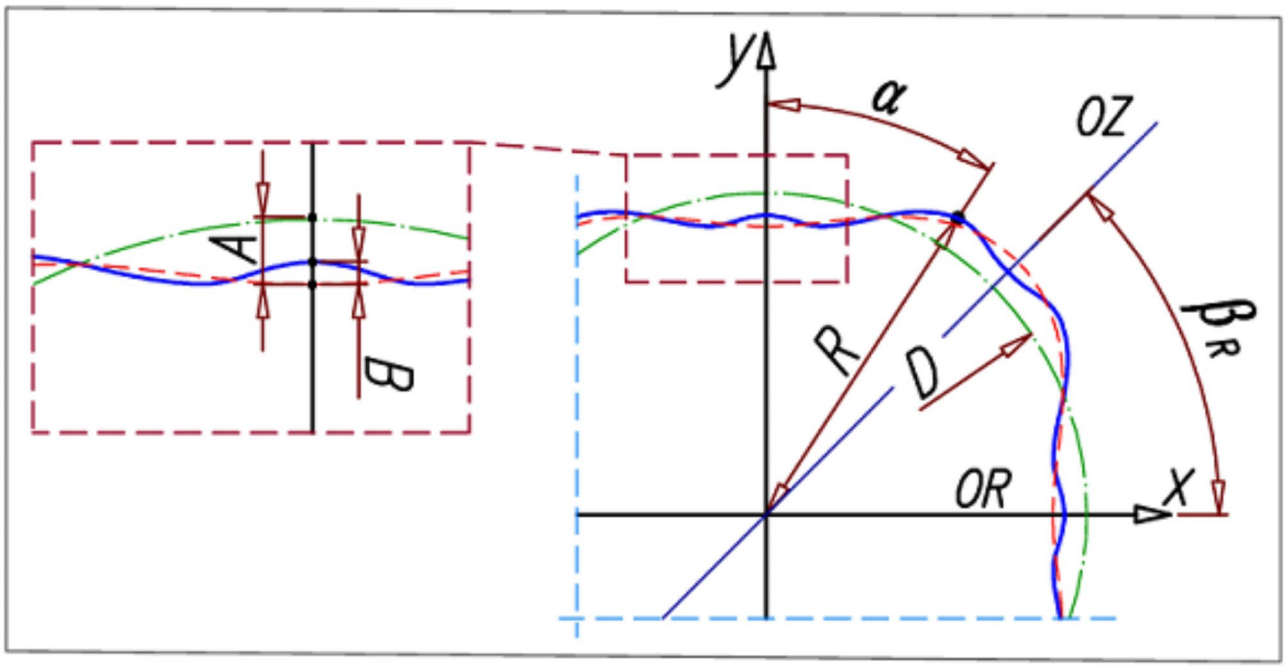

Fig. 4. Parameters of the rolling line of the rotor of the 4×6 type mechanism: OZ – axis of symmetry of the hump lift, OR – axis of symmetry of the hump rebate, D – diameter of the base circle of the rotor, A, B – amplitudes of the cosine function (formula (1)), R – radius of the rotor corresponding to the angle α (formula (1)). (created in Autodesk Autocad 2024, https://www.autodesk.com/)

n_R	n_E	z_S	z_R	z_E
4	6	10	44	66
β_E	β_R	A	B	D
30°	45°	1.937 mm	0.339 mm	31.0 mm
m	A_{ch-min}	A_{ch-max}	H	q_g
0.75 mm	23.96 mm^2	76.38 mm^2	15 mm	18.87 cm^3/rev.

Table 1. Basic parameters of the satellite mechanisms.

Volume of the working chambers

In satellite mechanisms the volume V_{ch} of the chamber changes as the rotor rotates from a value of V_{ch-min} to a value of V_{ch-max}. These volumes are expressed by the formulae[33,34]:

$$V_{ch-max} = H \cdot A_{ch-max} \tag{5}$$

$$V_{ch-min} = H \cdot A_{ch-min} \tag{6}$$

The total change in the volume of the working chamber is therefore[33,34]:

$$\Delta V_{ch} = H \cdot (A_{ch-max} - A_{ch-min}) \tag{7}$$

The change in working volume ΔV_{ch} from V_{ch-min} to V_{ch-max} take place over the following range of the rotor angle of rotation:

$$\alpha_{R-A} = \beta_E + \beta_R = \frac{n_{ch}}{n_E \cdot n_R} \cdot 180^o \tag{8}$$

However, the entire cycle of the change in chamber volume, i.e. from V_{ch-min} through V_{ch-max} to V_{ch-min} takes place within the angle range:

$$\alpha_{R-B} = 2 \cdot \alpha_{R-A} \tag{9}$$

During one complete rotation of the shaft ($\alpha_R = 360°$), the one working chamber therefore performs the following number of filling and emptying cycles:

$$n_{ER} = \frac{360^o}{\alpha_{R-B}} = \frac{n_E \cdot n_R}{n_{ch}} \tag{10}$$

If during the rotation of the rotor, each working chamber changes its volume from V_{ch-min} to V_{ch-max} (formula (7)), then the number n_{vc} of cycles of volume change of all working chambers during one complete rotation of the rotor (360° rotation) is as follows:

$$n_{vc} = n_{ER} \cdot n_{vh} = n_E \cdot n_R \tag{11}$$

The total volume change of all working chambers per one full rotation of the shaft ($\alpha_R = 360°$) is therefore:

$$q_g = n_{vc} \cdot \Delta V_{ch} \quad \left[m^3/rev\right] \tag{12}$$

The geometric working volume q_g of the mechanism is, therefore, a constant value and does not depend on the angle of rotation α_R of the rotor (shaft) of the machine, but only depends on the number n_{vc} of cycles of volume changes of all working chambers and on the difference between the maximum and minimum volume of the working chamber. Formulae (11) and (12), but without proof, have already been described in earlier publications, e.g. in[33,34].

The start of the filling of each successive chamber (e.g. chamber I next to chamber II – Fig. 3) occurs after the rotor has turned through an angle of:

$$\alpha_{R-2} = \beta_E = \frac{1}{n_E} \cdot 360^o \tag{13}$$

According to[34,54], it is assumed that the field of the chamber for the angle of rotation of the rotor $\alpha_R = 0$ has a minimum value, i.e. A_{ch-min}. Therefore, for the field A_{ch} of the working chamber $\alpha_R \geq 0$ changes its value depending on the rotor rotation angle α_R according to[34,54]:

$$A_{ch} = 0.5 \cdot (A_{ch-max} - A_{ch-min}) \cdot (1 - \cos(\alpha_R \cdot n_{ER})) + A_{ch-min} \tag{14}$$

Therefore, the volume V_{ch} of the working chamber also changes depending on the rotor rotation angle α_R, i.e.:

$$V_{ch} = H \cdot A_{ch} \tag{15}$$

So, if:

a. $\alpha_R \in \left(\frac{k}{n_{ER}} \cdot 360^o; \frac{2 \cdot k+1}{n_{ER}} \cdot 180^o\right)$, where k = 0,1,2,…. – an increase in the chamber volume takes place, i.e. a filling process;
b. $\alpha_R \in \left(\frac{2 \cdot k+1}{n_{ER}} \cdot 180^o; \frac{k+1}{n_{ER}} \cdot 360^o\right)$ – a reduction in the chamber volume takes place, i.e. an emptying process;
c. $\alpha_R = \frac{k}{n_{ER}} \cdot 360^o$ – the volume of the working chamber is minimal (V_{ch-min});
d. $\alpha_R = \frac{2 \cdot k+1}{n_{ER}} \cdot 180^o$ – the volume of the working chamber is maximal (V_{ch-max}).

Figure 5 shows the characteristics of the volume of the one working chamber of the satellite mechanism as a function of the angle of rotation α_R of the rotor determined according to formulas (14) and (15).

Formula (15) can be generalized for each chamber. This means that the volume of the working chamber with the number 'i_{ch}' for a certain angle of rotation α_R of the rotor is:

$$V_{ch(i_{ch})} = H \cdot [0.5 \cdot (A_{ch-max} - A_{ch-min}) \cdot [1 - \cos((\alpha_R - 2 \cdot \beta_R \cdot (i_{ch} - 1)) \cdot n_{ER})] + A_{ch-min}] \tag{16}$$

Figure 6 shows the volume characteristics of all working chambers of the satellite mechanism as a function of the rotor rotation angle α_R, which is determined according to Eq. (16).

The sum of the volumes of all working chambers assumes a certain value, i.e.:

$$V = \sum_{i_{ch}=1}^{n_{ch}} V_{ch(i_{ich})} = 0.5 \cdot H \cdot n_{ch} \cdot (A_{ch-max} + A_{ch-min}) \tag{17}$$

This means that the sum of the volumes of all the working chambers of the satellite mechanism is constant and independent of the angle of rotation α_R of the shaft. For the satellite mechanism considered here, it is V = 13.045 cm^3.

The volumes V_{sm-in} of all filled chambers and the volumes V_{sm-out} of all emptied chambers can be calculated according to relationships (16) and (17), provided that:

a. for filled chambers:

$$\alpha_R \in \left(\frac{k}{n_{ER}} \cdot 360^o + \beta_E \cdot (i_{ch} - 1) \cdot (k+1); \frac{2 \cdot k+1}{n_{ER}} \cdot 180^o + \beta_E \cdot (i_{ch} - 1) \cdot (k+1)\right) \tag{18}$$

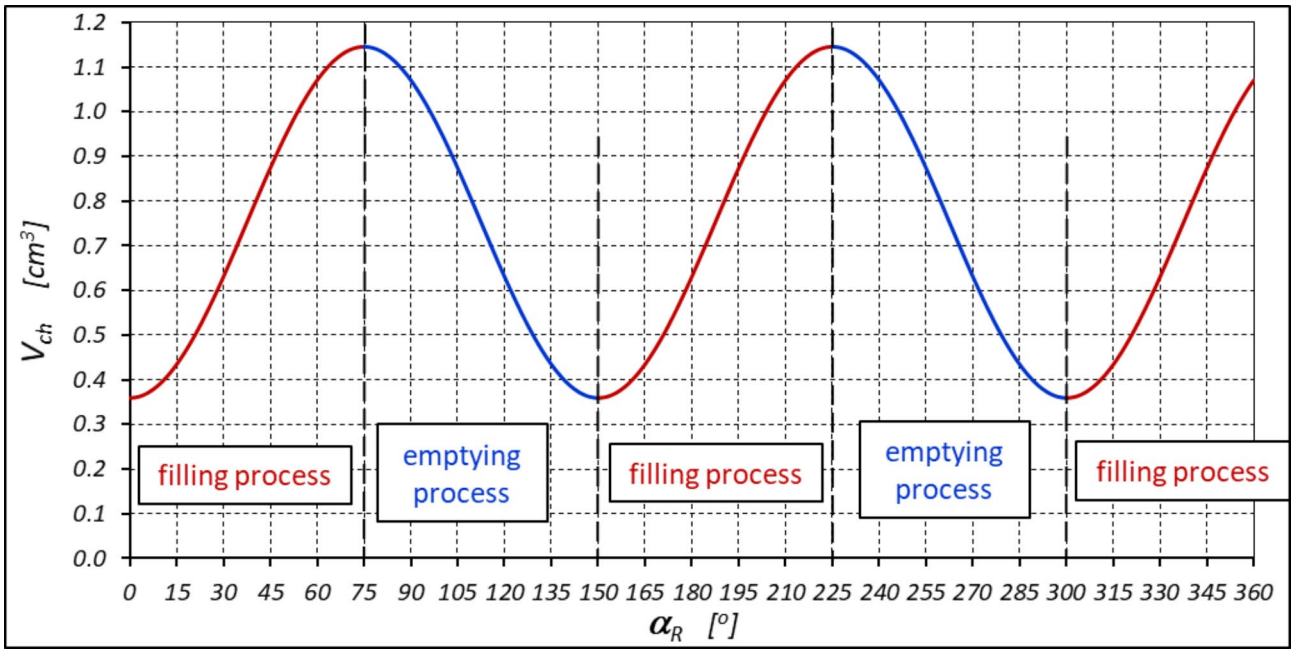

Fig. 5. The volume V_{ch} of the working chamber of the satellite mechanism as a function of the angle of rotation α_R of the rotor (within one complete rotation of the rotor – $\alpha_R = 360°$).

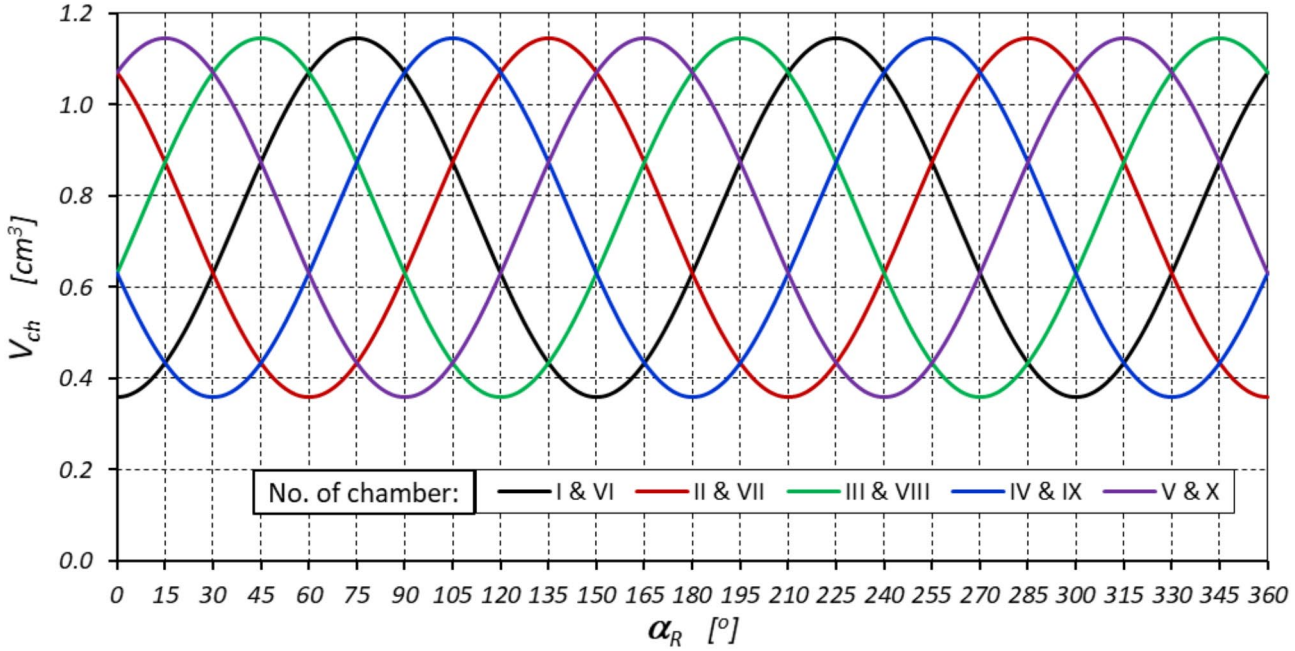

Fig. 6. Characteristics of the volume V_{ch} of the working chambers of the satellite mechanism as a function of the angle of rotation α_R of the rotor (within one complete rotation of the rotor – $\alpha_R = 360°$).

b. for emptied chambers:

$$\alpha_R \in \left(\frac{2 \cdot k+1}{n_{ER}} \cdot 180^o + \beta_E \cdot (i_{ch}-1) \cdot (k+1); \left(\frac{360^o}{n_{ER}} + \beta_E \cdot (i_{ch}-1)\right) \cdot (k+1)^2\right) \quad (19)$$

For the satellite mechanism under consideration, the characteristics of V_{sm-in} and V_{sm-out} are shown in Figs. 9 and 10 respectively. These figures show the number of chamber that reach the minimum volume V_{ch-min} (highlighted in yellow) and the maximum volume V_{ch-max} (highlighted in green).

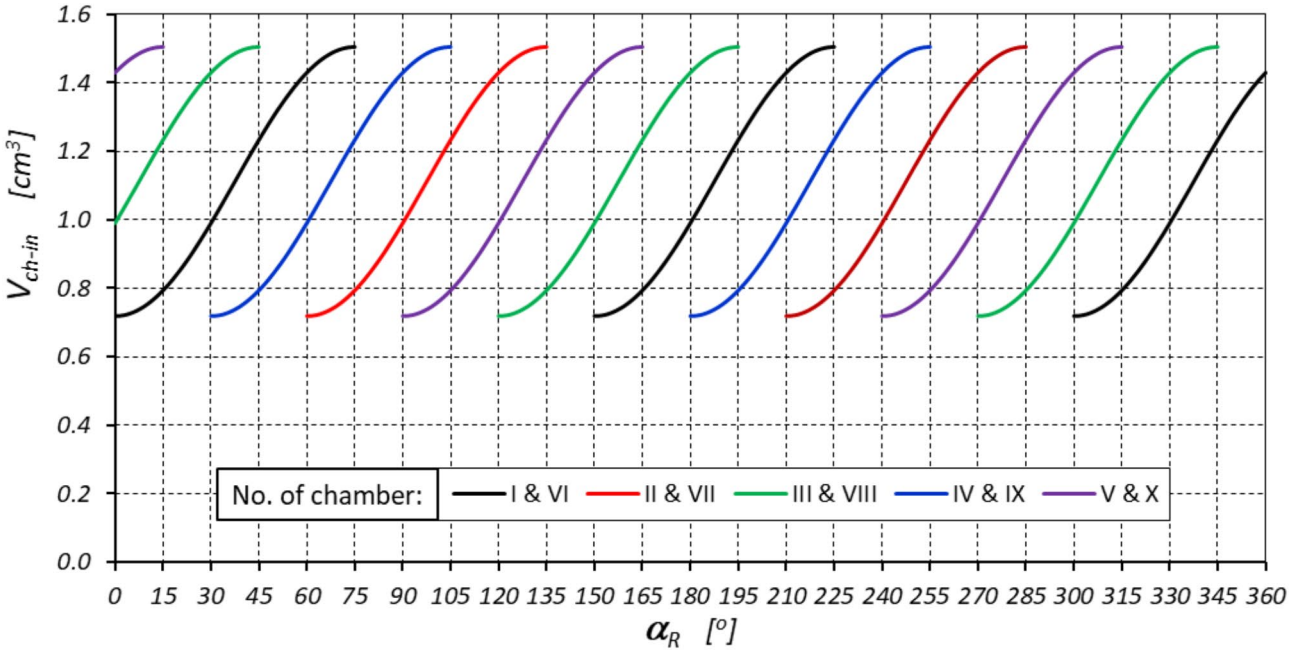

Fig. 7. Characteristics of the volume $V_{ch\text{-}in}$ of the chambers with increasing volume (filled) as a function of the angle of rotation α_R of the rotor (within one complete rotation of the rotor – $\alpha_R = 360°$

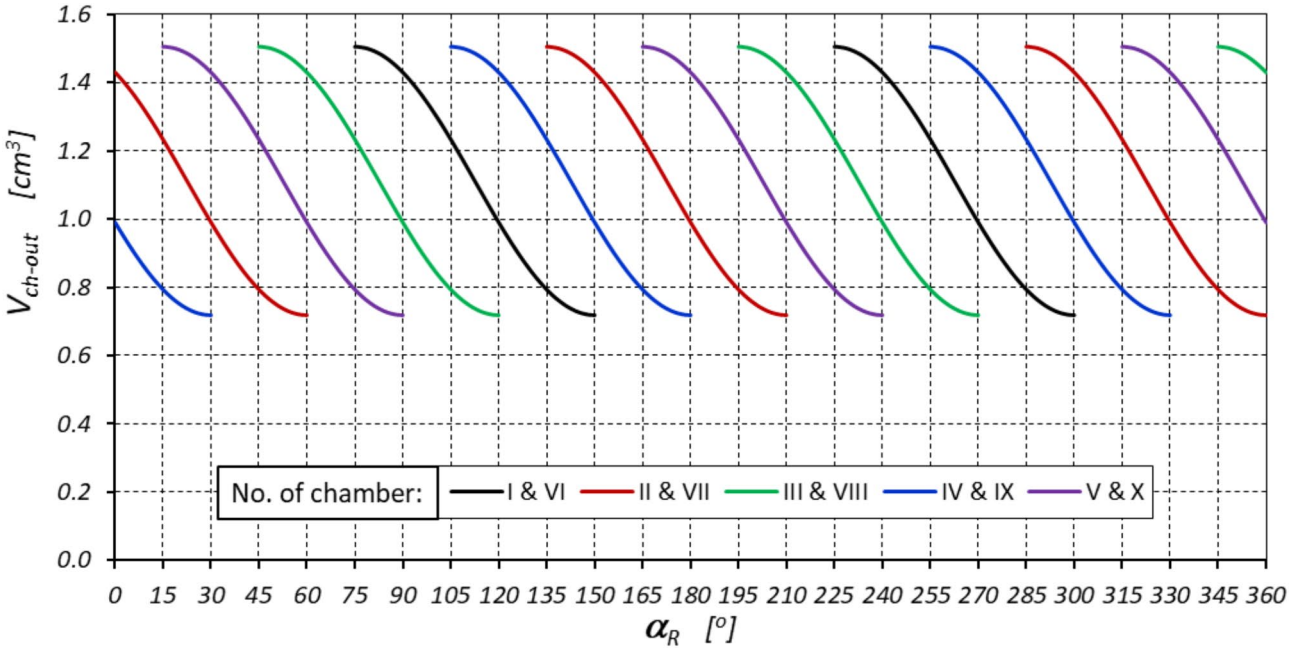

Fig. 8. Characteristics of the volume $V_{ch\text{-}out}$ of the chambers with decreasing volume (emptied) as a function of the angle of rotation α_R of the rotor (within one complete rotation of the rotor – $\alpha_R = 360°$).

From Figs. 7, 8, 9 and 10 it can be concluded that either four or six chambers are filled or emptied simultaneously during both filling and emptying. The number n_{ch-in} of filled chambers and the number n_{ch-out} of emptied chambers correspond to the number n_R of humps of the rotor or the number n_E of humps of the bypass, i.e.: $n_{ch-in} = n_{ch-out} = n_R$ or $n_{ch-in} = n_{ch-out} = n_E$. Therefore, for each angle of rotation α_R of the shaft the following relations is true:

$$n_{ch} = n_{ch-in} + n_{ch-out} + n_{ch-d} \tag{20}$$

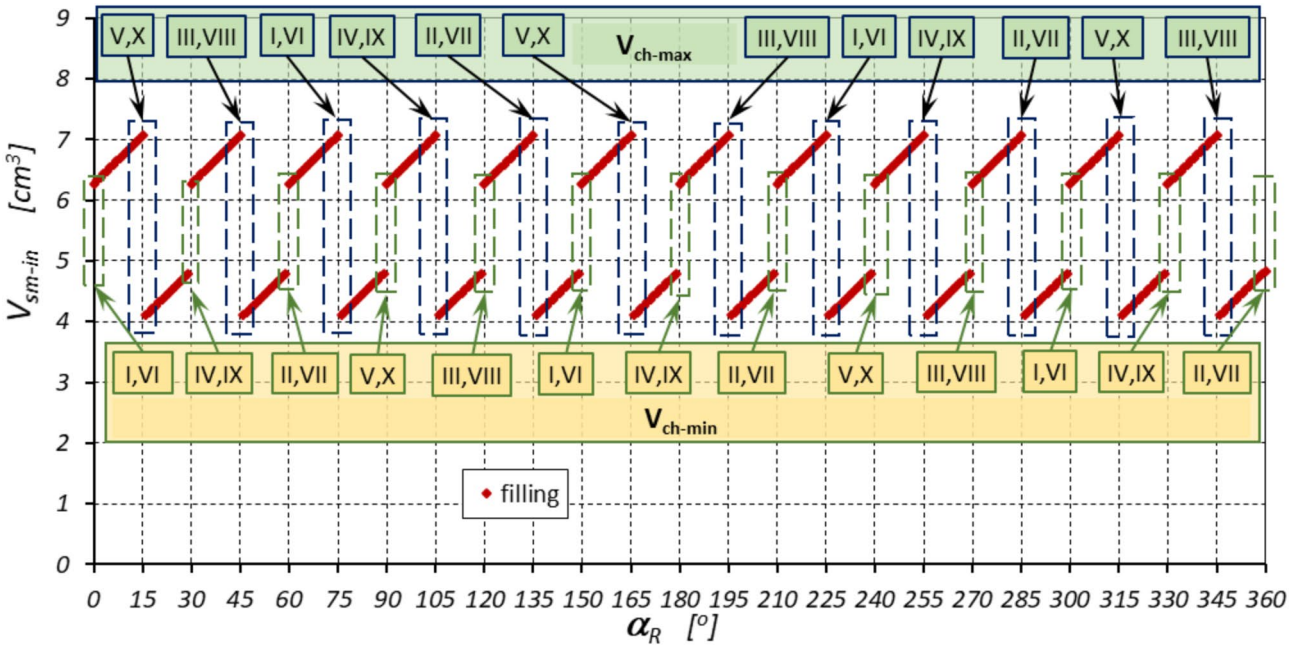

Fig. 9. Volume V_{sm-in} of the filled working chambers as a function of the angle of rotation α_R of the rotor (within one complete rotation of the rotor – $\alpha_R = 360°$).

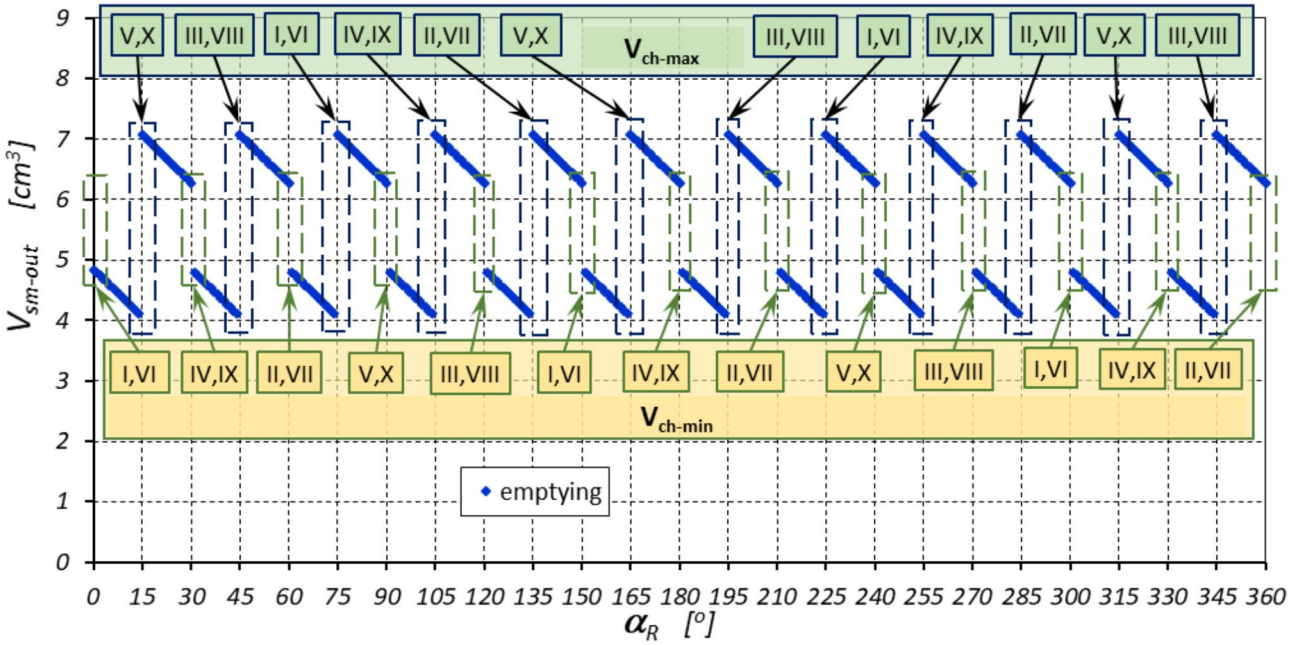

Fig. 10. Volume V_{sm-out} of the emptied working chambers as a function of the angle of rotation α_R of the rotor (within one complete rotation of the rotor – $\alpha_R = 360°$).

where n_{ch-d} is the number of dead chambers (i.e. the number of chambers with a maximum volume V_{ch-max} or a minimum volume V_{ch-min}):

$$n_{ch-d} = n_C - n_R \tag{21}$$

For example:

1. for each angle $\alpha_R \in (0;15°)$:

- six chambers are filled simultaneously, i.e. chambers I, III, V, VI, VIII and X;
- four chambers are emptied simultaneously, i.e. chambers II, IV, VII and IX;

2. for each angle $\alpha_R \in (15°;30°)$:

- only four chambers are filled simultaneously, i.e. chambers I, III, VI and VIII;
- six chambers are emptied simultaneously, i.e. chambers II, IV, V, VII, IX and X.

Flow rate in the satellite mechanism.

The flow rate Q_{ch} in the one working chamber (the so-called absorption capacity of the working chamber) is:

$$Q_{ch} = \frac{dV_{ch}}{d\tau} = H \cdot \omega \cdot \frac{dA_{ch}}{d\alpha_R} \tag{22}$$

where ω is the angular velocity of the shaft (rotor). Therefore:

$$Q_{ch} = 0.5 \cdot H \cdot \omega \cdot (A_{ch-max} - A_{ch-min}) \cdot n_{ER} \cdot \sin(\alpha_R \cdot n_{ER}) \tag{23}$$

Figure 11 shows the flow rate Q_{ch} in the one working chamber as a function of the angle of rotation α_R of the rotor, calculated according to formula (23).

For any chamber with the number i_{ch}, for a given angle of rotation α_R of the rotor, the above formula (23) takes the form:

$$Q_{ch(i_{ch})} = 0.5 \cdot H \cdot \omega \cdot (A_{ch-max} - A_{ch-min}) \cdot n_{ER} \cdot \cos((\alpha_R - 2 \cdot \beta_R \cdot (i_{ch} - 1)) \cdot n_{ER}) \tag{24}$$

Formulae (23) and (24) describe the flow rate of the liquid booth in the process of filling chambers (positive values of Q_{ch}, i.e.: $Q_{ch} > 0$) and in the process of emptying chambers (negative values of Q_{ch}, i.e.: $Q_{ch} < 0$). The process of filling the chambers takes place when the angle of rotation α_R of the shaft fulfills the condition given in formula (18). The process of emptying the chambers takes place if the angle of rotation α_R of the shaft fulfills the condition given in formula (19). Figures 12 and 13 show the liquid flow rate $Q_{ch\text{-}in}$ in the filled chambers and the liquid flow rate $Q_{ch\text{-}out}$ in the emptied chambers, respectively.

The total flow rate Q_{ms} in the working mechanism is zero, i.e.:

$$Q_{ms} = \sum_{i_{ch}=1}^{n_{ch}} Q_{ch(i_{ich})} = 0 \tag{25}$$

The basic quantity defined in the theory of positive displacement machines is the delivery or absorptivity. The term delivery refers to pumps and denotes the volumetric quantity of liquid pumped by the pump per unit time (output flow rate)[47]. In contrast, the term absorptivity refers to motors and also denotes the volumetric quantity of liquid but absorbed by the motor per unit of time (derived inlet flow rate)[46,50]. Therefore, Eq. (25) cannot be a

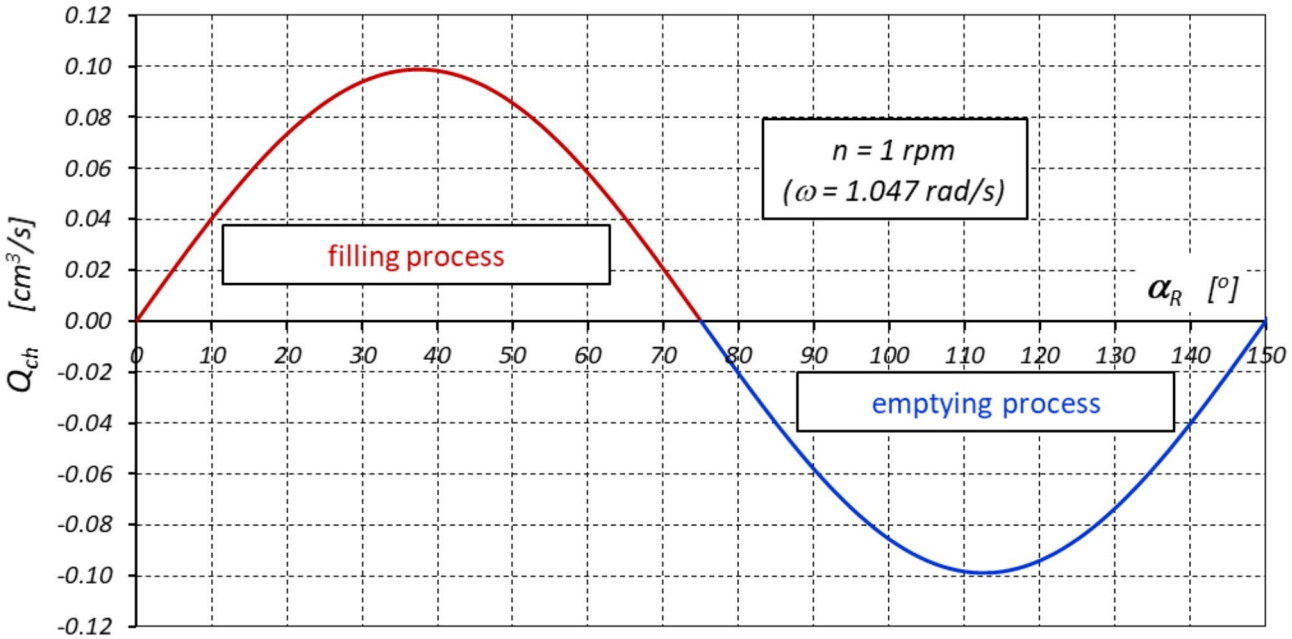

Fig. 11. Characteristics of the flow rate Q_{ch} in the one working chamber as a function of the angle of rotation α_R of the rotor (shaft).

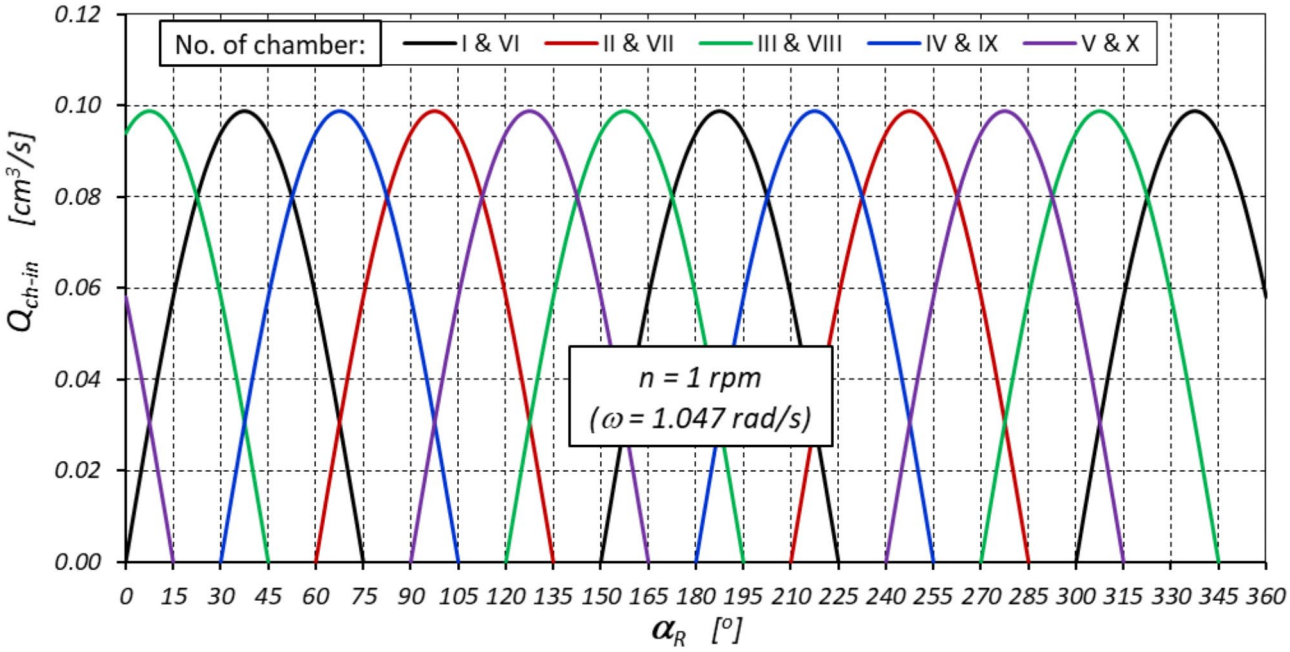

Fig. 12. Characteristics of the liquid flow rate $Q_{ch\text{-}in}$ in the filled chambers as a function of the angle of rotation α_R of the rotor (within one complete rotation of the rotor – $\alpha_R = 360°$).

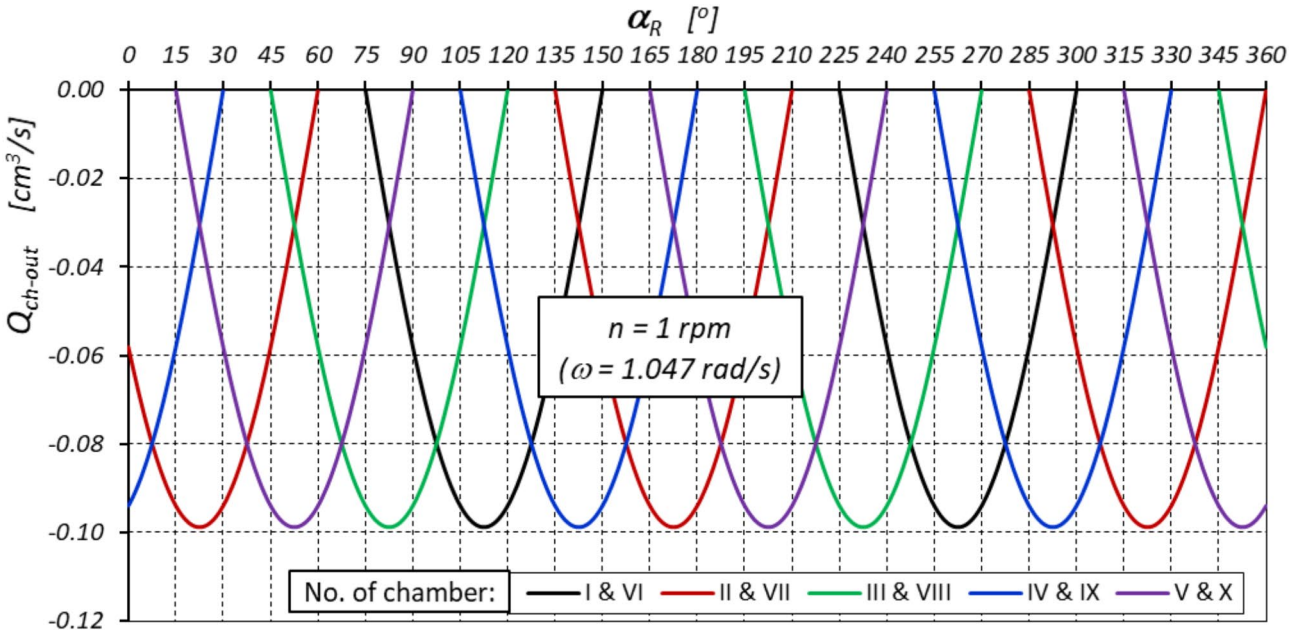

Fig. 13. Characteristics of the liquid flow rate $Q_{ch\text{-}out}$ in the emptied chambers as a function of the angle of rotation α_R of the rotor (within one complete rotation of the rotor – $\alpha_R = 360°$).

definition of the delivery or absorptivity of a satellite mechanism. The delivery or absorptivity Q_i of the satellite mechanism should therefore be defined on the basis of formula (24) as:

a. for $\cos\left((\alpha_R - \beta_E \cdot (i_{ch} - 1)) \cdot n_{ER}\right) \geq 0$:

$$Q_i = \sum_{i_{ch}=1}^{n_{ch}} Q_{ch(i_{ich})} \tag{26}$$

b. for $\cos\left((\alpha_R - \beta_E \cdot (i_{ch} - 1)) \cdot n_{ER}\right) \leq 0$:

$$Q_i = \sum_{i_{ch}=1}^{n_{ch}} \left| Q_{ch(i_{ich})} \right| \tag{27}$$

Since the flow in the one working chamber depends on the angle of rotation α_R of the shaft (formula (24)) formulas (26) and (27) define the instantaneous flow rate Q_i in the entire working mechanism. The instantaneous value of Q_i changes from the minimum value Q_{i-min} to the maximum value Q_{i-max}. The number of cycles of change from Q_{i-min} to Q_{i-max} is equal to the number n_{vc} (formula (11)). The flow rates Q_i, Q_{i-min}, Q_{i-max}, and Q for the satellite mechanism operating as a pump (at a constant angular velocity of the shaft $\omega = 1.047$ rad/s) are shown in Fig. 14.

The instantaneous geometric working volume

The flow rate Q in a positive displacement machine is also defined as[26,33,34,54]:

$$Q = q_g \cdot n = \frac{30}{\pi} \cdot q_g \cdot \omega \tag{28}$$

where n is the rotational speed of the shaft (rotor) in [rpm] and the geometric working volume q_g is described by formula (12). The geometric working volume q_g is assumed to be a constant value that is independent of the angle α_R of rotation of the shaft. However, a comparison of formulae (24), (26) (or (27)) and (28)) shows something different. This means that the geometric working volume of the mechanism changes its value depending on the angle of rotation α_R of the shaft. This means that for each angle of rotation α_R of the shaft, there is an instantaneous value q_{gi} of the geometric working volume. This value can be calculated by shifting and transforming the formulae (24), (26) and (28) accordingly, i.e.:

$$q_{gi} = \frac{\pi}{60} \cdot H \cdot (A_{ch-max} - A_{ch-min}) \cdot n_{ER} \cdot \sum_{i_{ch-in}=1}^{n_{ch-in}} \cos\left((\alpha_R - \beta_E \cdot (i_{ch-in} - 1)) \cdot n_{ER}\right) \tag{29}$$

where i_{ch-in} is the number of the filling chamber. Thus, it can be concluded that the geometric working volume q_g is the average of the instantaneous geometric working volumes q_{gi}:

$$q_g = \frac{1}{k_i} \cdot \sum_{k_i=1}^{k_i=x_i} q_{gi(k_i)} = const. \tag{30}$$

where $k_i = 1,2,\ldots,x_i$ is the number of values q_{gi} from a specific interval of the angle of rotation α_R of the shaft. It can be seen from Fig. 14 that the values of q_{gi} should be calculated for angles of rotation α_R of the shaft from any interval $\frac{360^o}{n_{vc}}$. The characteristics of the instantaneous geometric working volume q_{gi} are shown in Fig. 15.

The results of the analyses prove that the instantaneous q_{gi} value of the geometric working volume varies from a minimum value of q_{gi-min} to a maximum value of q_{gi-max} depending on the angle of rotation α_R of the shaft. The value of q_{gi-max} occurs when in the formula (29) the term $\sum_{i_{ch-in}=1}^{n_{ch-in}} \cos\left((\alpha_R - \beta_E \cdot (i_{ch-in} - 1)) \cdot n_{ER}\right) = max.$

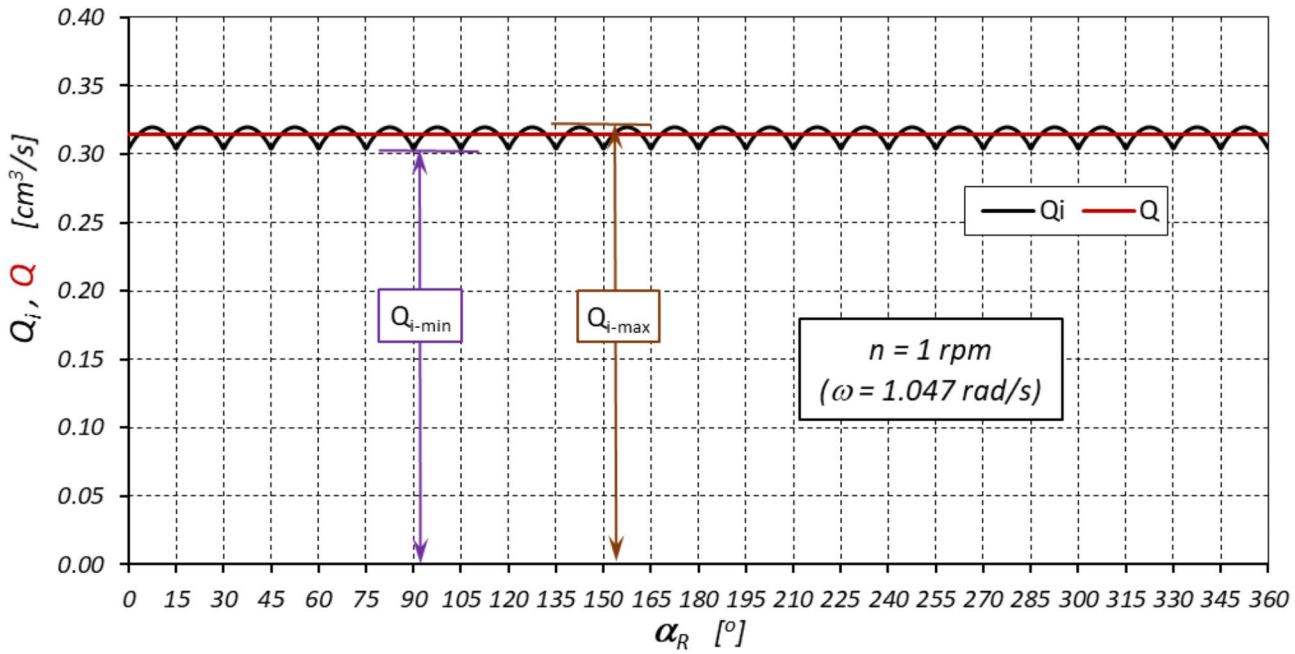

Fig. 14. Characteristics of instantaneous flow rate Q_i and average flow rate Q in the satellite mechanism as a function of the angle of rotation α_R of the rotor (within one complete rotation of the rotor – $\alpha_R = 360°$).

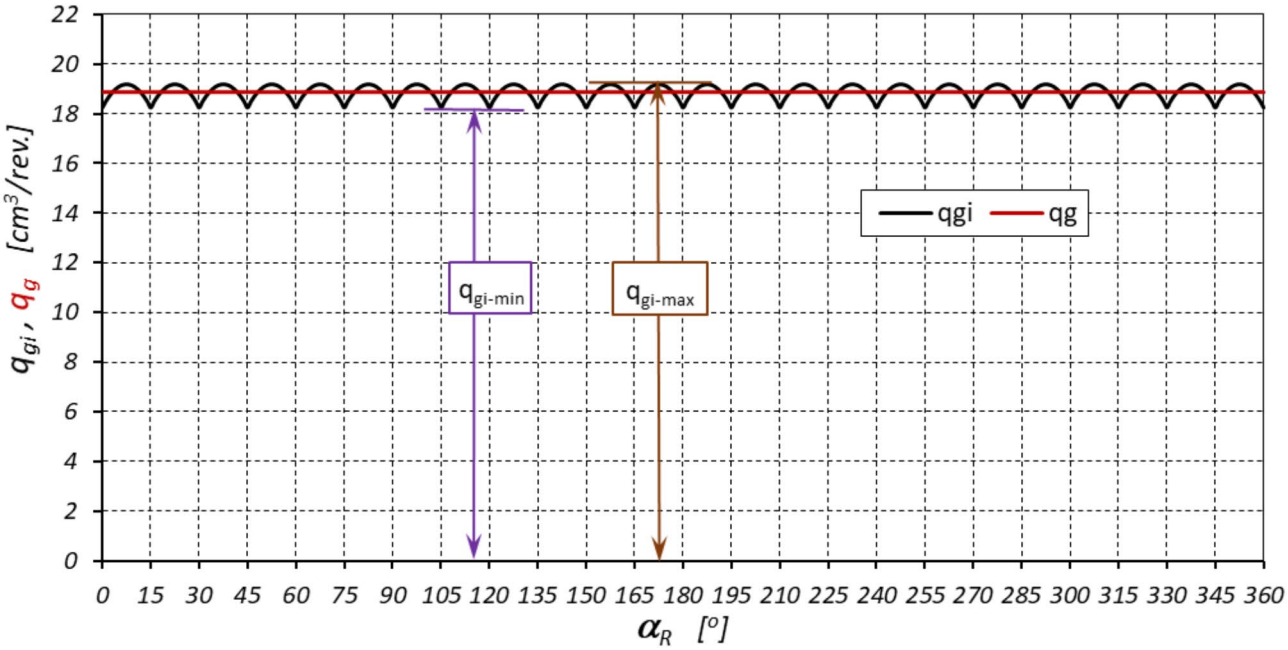

Fig. 15. Characteristics of the instantaneous geometric working volume q_{gi} and the average geometric working volume q_g of the satellite mechanism as a function of the angle of rotation α_R of the rotor (within one complete rotation of the rotor – $\alpha_R = 360°$).

, while the value q_{gi-min} takes place if $\sum_{i_{ch-in}=1}^{n_{ch-in}} \cos\left((\alpha_R - \beta_E \cdot (i_{ch-in} - 1)) \cdot n_{ER}\right) = min$. From the characteristics shown in Fig. 15, it can be seen that the value of q_{gi-min} occurs for $\alpha_R = k \cdot \frac{360^o}{n_{ER}}$, while the vsalue q_{gi-max} takes place for $\alpha_R = \frac{180^o}{n_{ER}} \cdot (1 + 2 \cdot k)$, where k = 0,1,2,…. The number of cycles of change from q_{gi-min} to q_{gi-max} is equal to the number of n_{vc} (formula (11)).

The instantaneous delivery of the pump and the irregularity (pulsation) of delivery

The rotational speed n of the shaft is the independent parameter for each positive displacement pump[47,48]. Therefore, if n = const. (ω = const.), the the geometric working volume q_g changes depending on the angle of rotation α_R of the shaft and thus the pump delivery changes also. In other words, the instantaneous delivery Q_i of the pump occurs (Fig. 14), that is :

$$Q_i = q_{gi} \cdot n \neq const. \tag{31}$$

A ssociated with the concept of instantaneous delivery Q_i of the pump is the concept of the irregularity δ_Q of the delivery of this pump (or, in other words, pulsation of the delivery of the pump), defined as[2,4]:

$$\delta_Q = 100 \cdot \frac{Q_{i-max} - Q_{i-min}}{Q} [\%] \tag{32}$$

Taking into account formulae (29), (30) and (31), the pulsation of the delivery can be defined as[32]:

$$\delta_Q = 100 \cdot \frac{q_{gi-max} - q_{gi-min}}{q_g} [\%] \tag{33}$$

The instantaneous rotational speed of the hydraulic motor and the irregularity (pulsation) of the rotational speed

The flow rate Q (absorption) is the independent parameter for each hydraulic motor[33,46,50]. So, if Q = const., the change in the geometric working volume q_g as a function of the angle of rotation α_R of the shaft leads to a change in the rotational speed of the shaft. In other words, the instantaneous rotational speed n_i of the motor shaft occurs, i.e.:

$$n_i = \frac{Q}{q_{gi}} \neq const. \tag{34}$$

From this, it can be concluded that the rotational speed n of the hydraulic motor shaft is the average of the instantaneous rotational speeds n_i:

$$n = \frac{1}{k_i} \cdot \sum_{k_i=1}^{k_i=x_i} n_{i(k_i)} = const. \tag{35}$$

where $k_i = 1,2,\ldots,x_i$ is the number of values q_{gi} from a specific interval of the angle of rotation α_R of the shaft. It can be seen from Fig. 14 that the values of n_i should be calculated for angles of rotation α_R of the shaft from any interval $\frac{360^o}{n_{vc}}$. The characteristics of the instantaneous rotational speed n_i and the average speed n at Q = const. are shown in Fig. 16.

Associated with the concept of instantaneous rotational speed n_i of the motor shaft is the concept of the irregularity δ_n of the motor rotational speed (or, in other words, pulsation of the motor rotational seed), defined as:

$$\delta_n = 100 \cdot \frac{n_{i-max} - n_{i-min}}{n} \, [\%] \tag{36}$$

Taking formulae (29), (30) and (34) into account, the pulsation of the rotational speed δ_n can be defined as:

$$\delta_n = 100 \cdot q_g \cdot \frac{q_{gi-max} - q_{gi-min}}{q_{gi-max} \cdot q_{gi-min}} \, [\%] \tag{37}$$

Torque on the pump shaft and irregularity (pulsation) of the torque

In hydraulic positive displacement machines without energy losses, the mechanical power is converted into hydraulic power (in the pump) or vice versa (in the motor)[2], i.e.:

$$q_g \cdot n \cdot (p_H - p_L) = 2 \cdot \pi \cdot M \cdot n \tag{38}$$

The relationship between the pressure difference in the working chambers and the torque on the shaft of the positive displacement machine is therefore as follows:

$$M = \frac{1}{2 \cdot \pi} \cdot q_g \cdot (p_H - p_L) \tag{39}$$

In the pump, the pressure p_H in the high-pressure working chamber HPC (Figs. 2 and 3) is the result of the hydraulic system load and the pressure drop in the internal channel of the pump connecting the HPC chamber to the external pump connection. On the other hand, the pressure p_L in the low-pressure working chamber LPC (Figs. 2 and 3) is the result of the pressure drop on the way from LPC chamber to the tank. The pressure increase in the pump is therefore a parameter independent of the pump. The torque M required to drive the pump is the effect of the pressure increase in this pump and depends on the geometric working volume q_g (formula (39)). Because the geometric working volume q_g assumes a constant value (q_g = const.), regardless of the angle

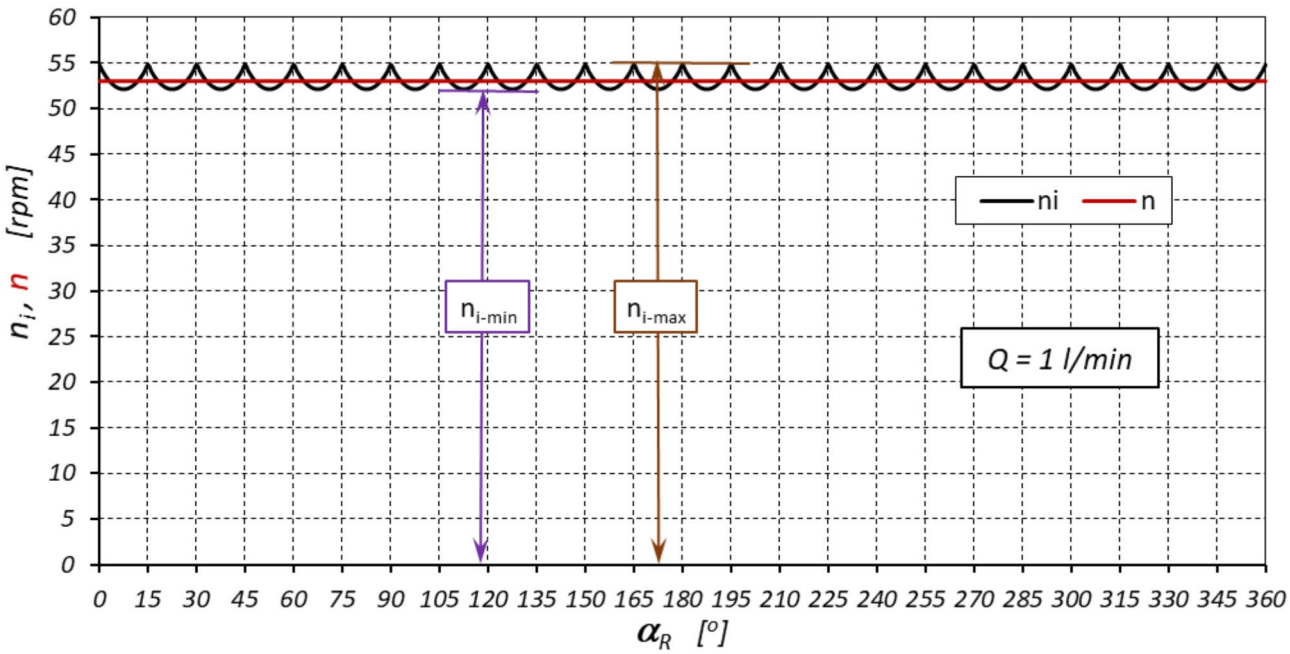

Fig. 16. Characteristics of instantaneous rotational speed n_i and the average rotational speed n of the rotor (shaft) as a function of the angle of rotation α_R of the rotor (within one complete rotation of the rotor – $\alpha_R = 360°$).

of rotation α_R of the shaft, the torque M on the pump shaft is also constant (M = const.) according to the above formula (39) and represents an average value.

The torque M required to drive the pump can also be determined as an average value of the values of the instantaneous torques M_i. The instantaneous torque M_i is the torque generated by the working mechanism for a certain angle of rotation α_R of the shaft (rotor). Therefore:

$$M = \frac{1}{k_j} \cdot \sum_{k_j=1}^{k_j=x_j} M_i \tag{40}$$

where $k_j = 1,2,3,\ldots,x_j$ is the number of values of the instantaneous torque M_i within one full rotation of the shaft.

In order to calculate the instantaneous values of the torque M_i on the pump shaft for given constant values of pressure p_H and p_L, it is necessary to calculate the values of the torque $M_{w(ich)}$ "generated" by each working chamber as a function of the angle of rotation α_R of the shaft. That is, the instantaneous torque M_i can be calculated as:

$$\overrightarrow{M_i} = \sum_{i_{ch}=1}^{n_{ch}} \overrightarrow{M_{w(i_{ch})}} = \overrightarrow{M_{i-HPC}} + \overrightarrow{M_{i-LPC}} \tag{41}$$

where:

- $\overrightarrow{M_{w(i_{ch})}}$ – the torque "generated" by the working chamber (numbered i_{ch}):

$$\overrightarrow{M_{w(i_{ch})}} = \overrightarrow{M_{w(i_{ch})-R}} + \underbrace{\overrightarrow{M_{w(i_{ch})-S1}} + \overrightarrow{M_{w(i_{ch})-S2}}}_{\overrightarrow{M_{w(i_{ch})-S}}} \tag{42}$$

- $\overrightarrow{M_{w(i_{ch})-R}}$ – the torque "generated" by the action of pressure in the chamber number i_{ch} on the rotor;
- $\overrightarrow{M_{w(i_{ch})-S1}}$ – the torque "generated" by the action of pressure in the chamber number i_{ch} on the first satellite;
- $\overrightarrow{M_{w(i_{ch})-S2}}$ – the torque "generated" by the action of pressure in the chamber number i_{ch} on the second satellite, adjacent to the first satellite;
- $\overrightarrow{M_{i-HPC}}$ – the torque "generated" by the high pressure p_H in all high-pressure chambers (HPC);
- $\overrightarrow{M_{i-LPC}}$ – the torque "generated" by the low pressure p_L in all low-pressure chambers (LPC).

The values of the torques mentioned above can be calculated as follows:

1. The torque "generated" by the rotor

$$M_{w(i_{ch})-R} = p_{(i_{ch})} \cdot H \cdot \int_{\propto=\propto_{(S1)}}^{\propto=\propto_{(S2)}} r_R \cdot R \cdot d\propto \tag{43}$$

where (Fig. 17):

- $p_{(ich)} = p_H$ or $p_{(ich)} = p_L$ – the pressure in the chamber with the number i_{ch};
- R – the radius of the rotor according to formula (1);
- r_R – the distance between the centre of rotation of the rotor (with the coordinates x_o,y_o) and the straight line defining the direction of the force dF_R (respectively $dF_{R\text{-}H}$ for the high-pressure chamber HPC and $dF_{R\text{-}L}$ for the low-pressure chamber LPC):

$$r_R = \sqrt{(x_F - x_o)^2 + (y_F - y_o)^2} \tag{44}$$

$$x_F = \frac{1}{2} \cdot \frac{\frac{y_{R1}-y_{R2}}{x_{R1}-x_{R2}} \cdot (x_{R1} + x_{R2}) + y_{R1} + y_{R2}}{\frac{y_{R1}-y_{R2}}{x_{R1}-x_{R2}} + \frac{x_{R1}-x_{R2}}{y_{R1}-y_{R2}}} \tag{45}$$

$$y_F = \frac{1}{2} \cdot \frac{x_{R1} + x_{R2} + \frac{x_{R1}-x_{R2}}{y_{R1}-y_{R2}} \cdot (y_{R1} + y_{R2})}{\frac{y_{R1}-y_{R2}}{x_{R1}-x_{R2}} + \frac{x_{R1}-x_{R2}}{y_{R1}-y_{R2}}} \tag{46}$$

- x_{R1}, y_{R1} and x_{R2}, y_{R2} – the coordinates of the points on the rotor for the angle α and for the angle α + dα respectively;
  the torque "generated" by the first satellite:

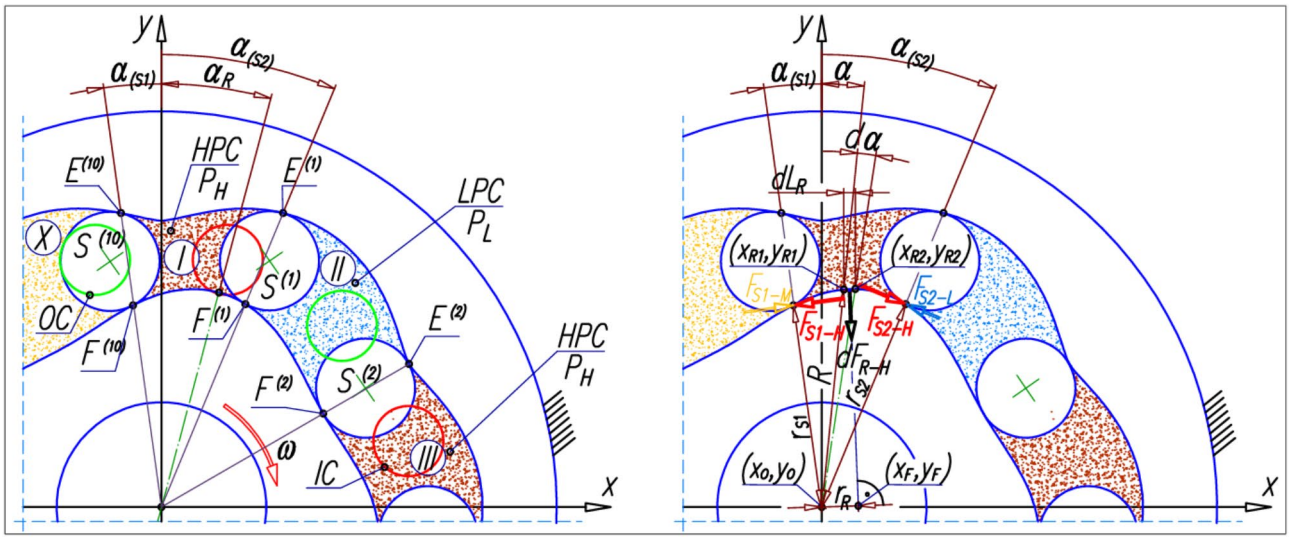

Fig. 17. The basic parameters of the satellite mechanism for calculating the torque. Description in the text. (created in Autodesk Autocad 2024, https://www.autodesk.com/)

$$M_{w(i_{ch})-S1} = \underbrace{\frac{1}{2} \cdot p_{(i_{ch})} \cdot H \cdot \sqrt{\left(x_{F(1)} - x_{E(1)}\right)^2 + \left(y_{F(1)} - y_{E(1)}\right)^2}}_{F_{S1}} \cdot r_{S1} \tag{47}$$

$$r_{S1} = \sqrt{(x_{F1} - x_o)^2 + (y_{F1} - y_o)^2} \tag{48}$$

where (Fig. 17):

- x_{F1} and y_{F1} – the coordinates of the point F located on the pitch line of the rotor and can be calculated using the formula (1) assuming $\alpha = \alpha_{(S1)}$;
- x_{E1} and y_{E1} – the coordinates calculated according to the method described in[15].

the torque "generated" by the second satellite:

$$M_{w(i_{ch})-S2} = \underbrace{\frac{1}{2} \cdot p_{(i_{ch})} \cdot H \cdot \sqrt{(x_{F2} - x_{E2})^2 + \left(y_{F2} - y_{E2}\right)^2}}_{F_{S2}} \cdot r_{S2} \tag{49}$$

$$r_{S2} = \sqrt{(x_{F2} - x_o)^2 + (y_{F2} - y_o)^2} \tag{50}$$

where (Fig. 17):

- x_{F2} and y_{F2} – the coordinates of the point F located on the pitch line of the rotor and can be calculated using formula (1) assuming $\alpha = \alpha_{(S2)}$;
- x_{E2} and y_{E2} – the coordinates calculated according to the method described in[15].

The characteristics of the torques $M_{w(1)-R}$, $M_{w(1)-S1}$, $M_{w(1)-S2}$, $M_{w(1)-S}$ and $M_{w(1)}$ "generated" by the pressure in the first working chamber (chamber No. I – i_{ch}=1) are shown in Figs. 18, 19 and 20.

Analysing the results of the torque calculations shows that in the satellite mechanism:

a. during the filling of the chamber (high pressure p_H) (Figs. 18 and 20):

- the maximum value of the torque "generated" by the rotor occurs for the angle of rotation of the shaft $\alpha_R = 180^o \cdot \left(\frac{1}{n_R} + k \cdot \frac{2}{n_{ER}}\right)$, where k = 0,1,2,…;
- the lowest value of the torque "generated" by the first satellite occurs for the angle of rotation of the shaft $\alpha_R = k \cdot \frac{360^o}{n_{ER}}$, where k = 0,1,2,…;
- the highest value of the torque "generated" by the second satellite occurs for the angle of rotation of the shaft $\alpha_R = 180^o \cdot \left(\frac{1}{n_E} + k \cdot \frac{2}{n_{ER}}\right)$, where k = 0,1,2,…;

b. during the emptying of the chamber (low pressure p_L) (Figs. 19 and 20):

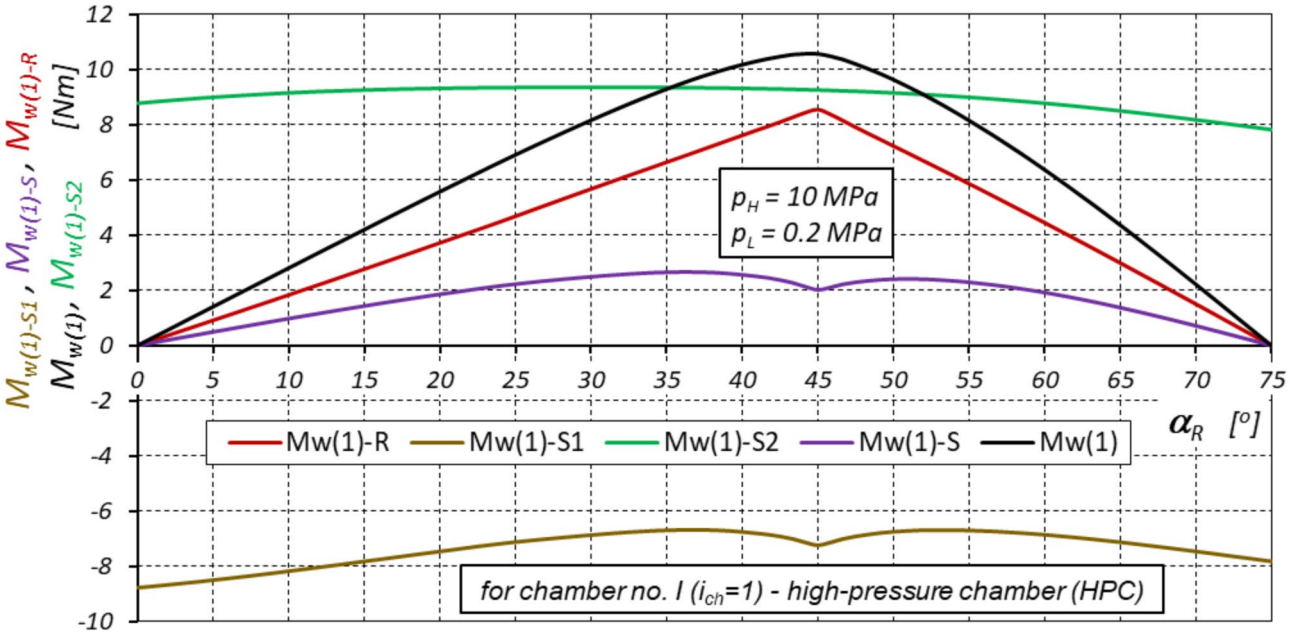

Fig. 18. Characteristics of the torque "generated" by working chamber No. I (i_{ch}=1) in the range of the shaft rotation angle α_R, which corresponds to the change in chamber volume from $V_{ch\text{-}min}$ to $V_{ch\text{-}max}$ (high pressure p_H in the chamber).

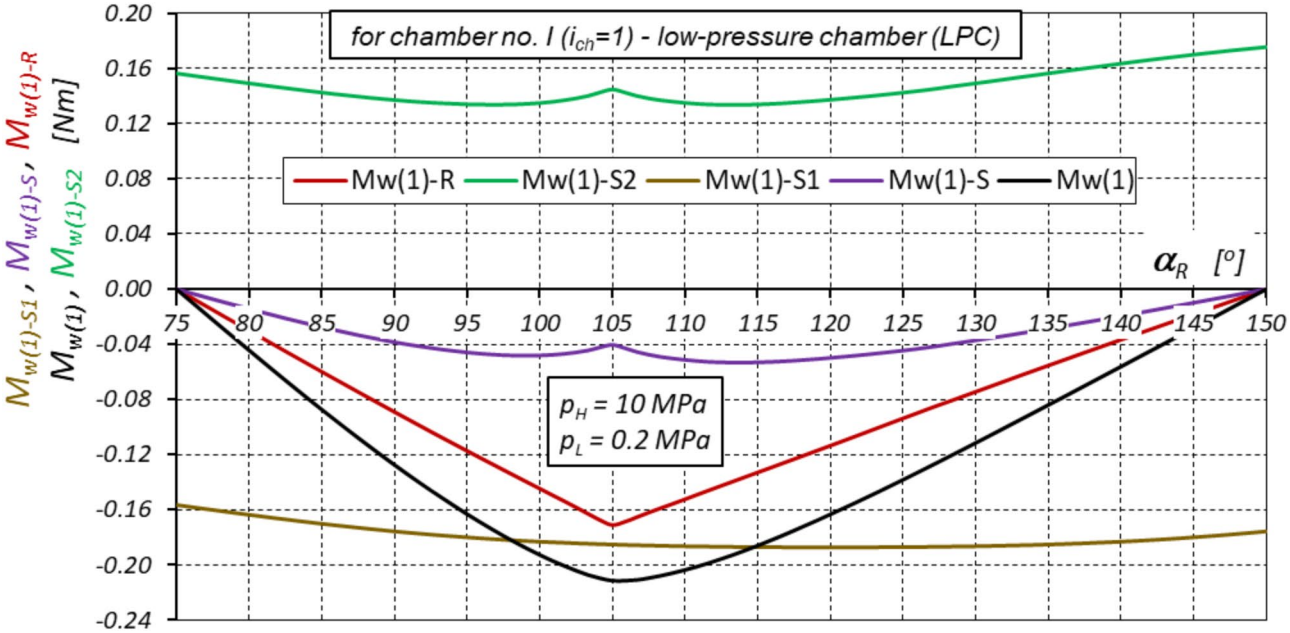

Fig. 19. Characteristics of the torque "generated" by working chamber No. I (i_{ch}=1) in the range of the shaft rotation angle α_R, which corresponds to the change in chamber volume from $V_{ch\text{-}max}$ to $V_{ch\text{-}min}$ (low pressure p_L in the chamber).

- the minimum value of the torque 'generated' by the rotor occurs for the angle of rotation of the shaft $\alpha_R = 180^o \cdot \left(\frac{1+2 \cdot k}{n_{ER}} + \frac{1}{n_E}\right)$, where k = 0,1,2,…;
- the lowest value of the torque 'generated' by the first satellite occurs for an angle of rotation of the shaft $\alpha_R = 360^o \cdot \left(\frac{2}{n_E} + k \cdot \frac{1}{n_{ER}}\right)$, where k = 0,1,2,…;
- the highest value of the torque 'generated' by the second satellite occurs for the angle of rotation of the shaft $\alpha_R = k \cdot \frac{360^o}{n_{ER}}$, where k = 0,1,2,….

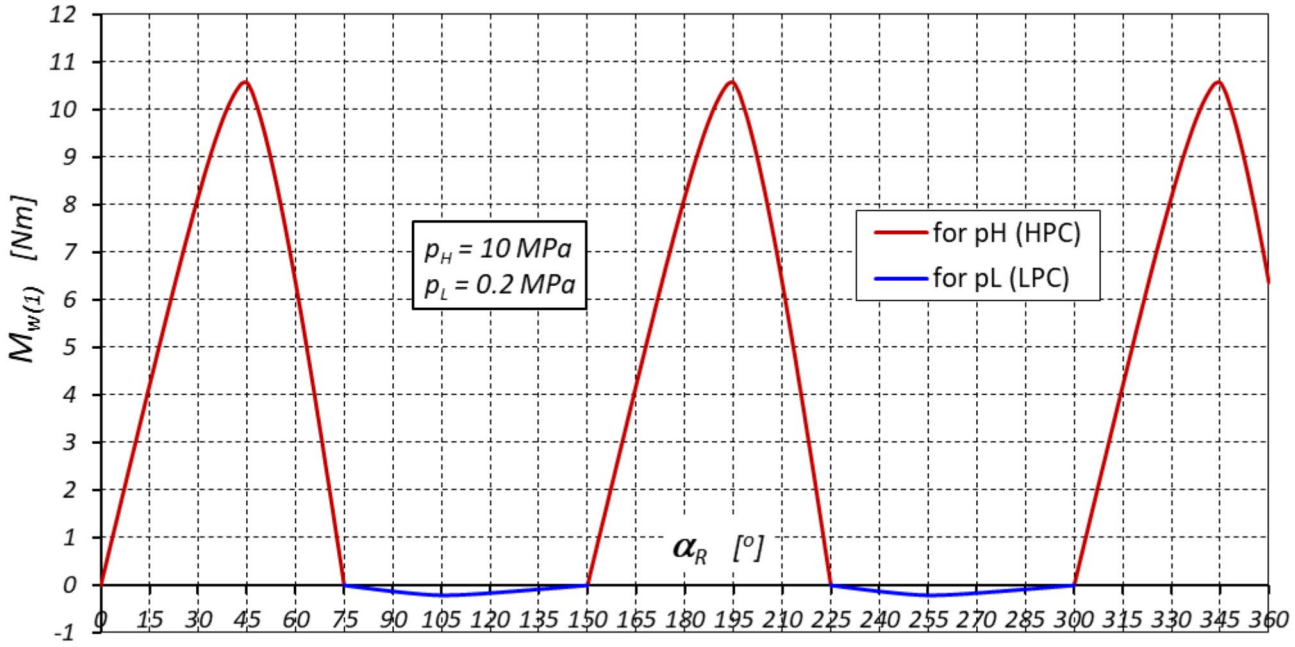

Fig. 20. Characteristics of the torque "generated" by the working chamber No. I (i_{ch}=1) as a function of the angle of rotation α_R of the rotor (within one complete rotation of the rotor – α_R = 360°).

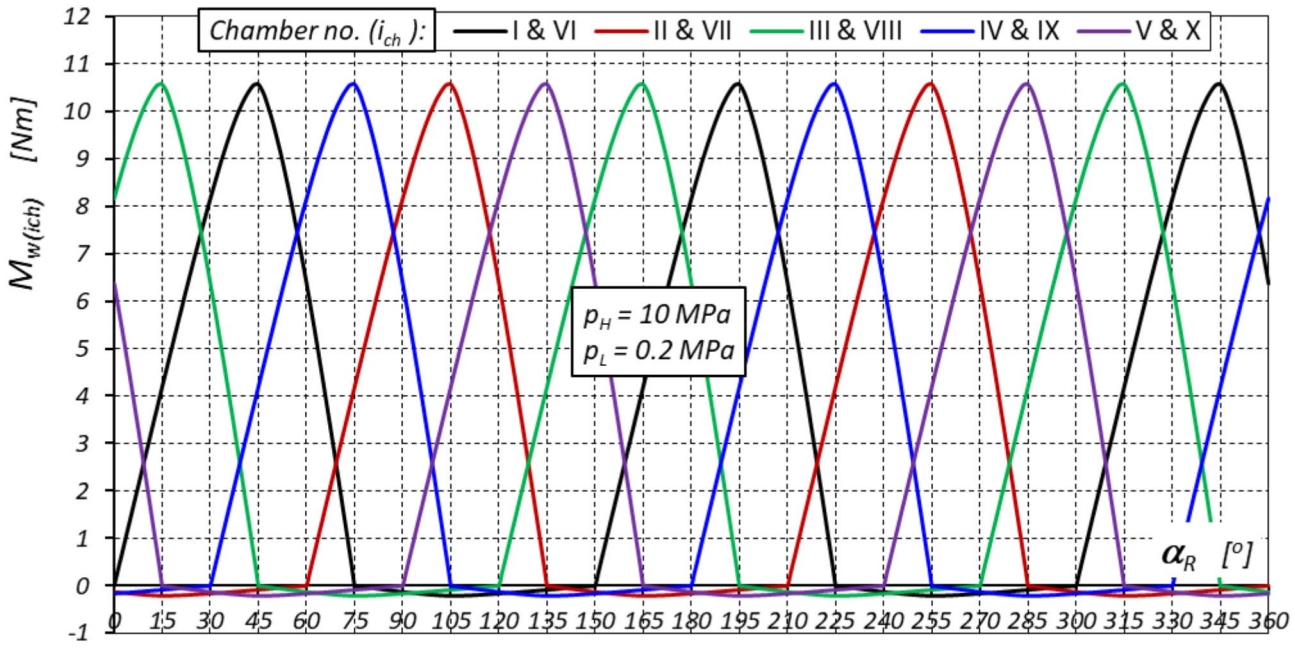

Fig. 21. Characteristics of the torque $M_{w(ich)}$ "generated" by all working chambers as a function of the angle of rotation α_R of the rotor (within one complete rotation of the rotor – α_R = 360°).

The characteristics of the torque "generated" by all working chambers of the satellite mechanism are shown in Fig. 21.

The torque "generated" by the one working chamber depends on the shaft rotation angle α_R. Consequently, the torque M_i expressed by formula (41) is also a function of the shaft rotation angle α_R. The instantaneous value of M_i varies from a minimum value of M_{i-min} to a maximum value of M_{i-max}. The number of cycles of change from M_{i-min} to M_{i-max} is equal to the number n_{vc} (formula (11)). Characteristics of the torques M_i, M_{i-min}, $M_{i-max,}$ and M "generated" in the satellite mechanism (pump operation) at a constant pressure increase in the mechanism ($\Delta p = p_H - p_L$ = 0.9 MPa) are shown in Fig. 22.

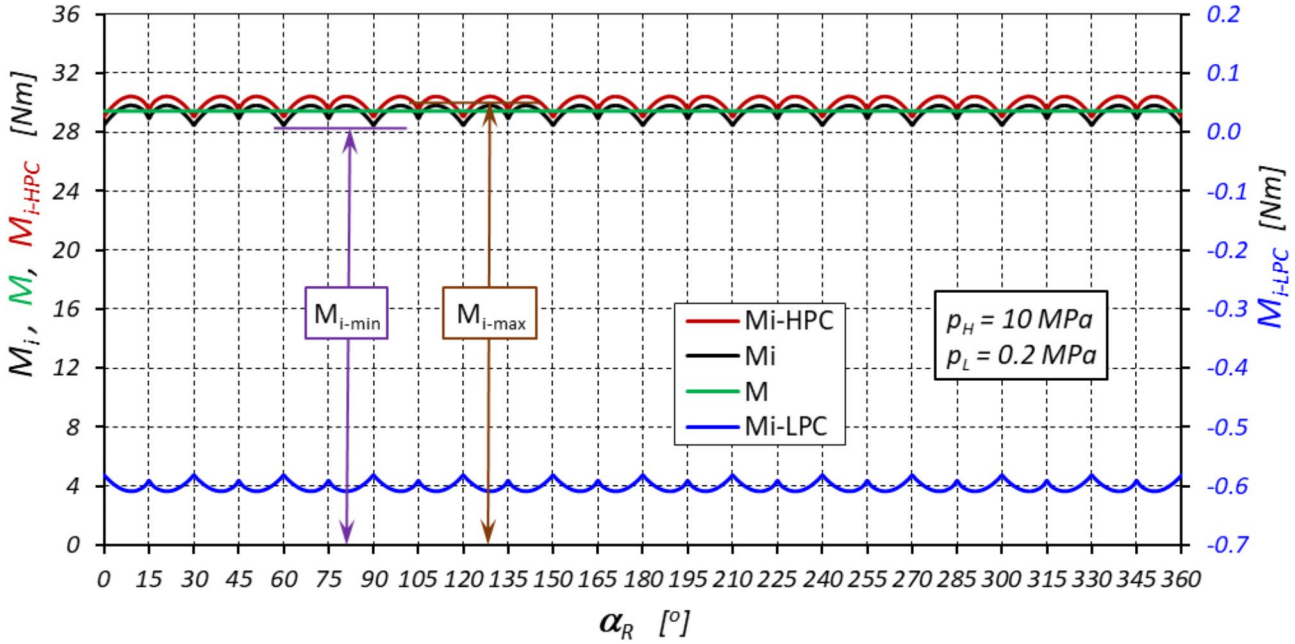

Fig. 22. Characteristics of the torque "generated" by the low-pressure working chambers ($M_{i\text{-}LPC}$) and the high-pressure working chambers ($M_{i\text{-}HPC}$). Characteristics of the instantaneous torque M_i and the average torque M as a function of the angle of rotation α_R of the rotor (within one complete rotation of the rotor – $\alpha_R = 360°$).

The results of the analyses show that the instantaneous value of the torque M_i is a function of the angle of rotation α_R of the shaft and varies from a minimum value of M_{i-min} to a maximum value of M_{i-max} (Fig. 22). The value M_{i-min} occurs for $\alpha_R = k \cdot \frac{180^o}{n_E}$, but the value M_{i-max} occurs for $\alpha_R = \frac{360^o}{(n_E+n_R)\cdot n_R} + k \cdot \beta_E$ and $\alpha_R = \frac{1}{2\cdot(n_E+n_R)} \cdot \left(\frac{180^o}{n_R} + n_R \cdot (\beta_R - \beta_E)\right) + k \cdot \beta_E$, where k=0,1,2,…. The number of cycles of change from M_{i-min} to M_{i-max} is equal to $\frac{n_{vc}}{2}$.

Associated with the concept of instantaneous torque M_i on the pump shaft is the concept of the torque irregularity δ_M (or in other words the pulsation of the torque), defined as:

$$\delta_M = 100 \cdot \frac{M_{i-max} - M_{i-min}}{M} \, [\%] \tag{51}$$

Since the value of the torque on the pump shaft changes from M_{i-min} to M_{i-max}, according to formula (39), for p_H = const. and p_L = const. there is a change in the working volume from $q_{gi(M)-min}$ to $q_{gi(M)-max}$. In contrast to the instantaneous geometric working volume q_{gi}, the working volume $q_{gi(M)}$ is referred to be called the instantaneous torque working volume.

The instantaneous torque working volume $q_{gi(M)}$ can therefore be determined from the calculated instantaneous torque M_i using formula (39) after a suitable transformation, i.e.:

$$q_{gi(M)} = 2 \cdot \pi \cdot \frac{M_i}{p_H - p_L} \tag{52}$$

Thus, it can be concluded that the torque working volume $q_{g(M)}$ is the average of the instantaneous working volumes $q_{gi(M)}$:

$$q_{g(M)} = \frac{1}{k_l} \cdot \sum_{k_l=1}^{k_l=x_l} q_{gi(k_i)} = const. \tag{53}$$

gdzie k_l = 1,2,…,x_l is the number of values of $q_{gi(M)}$ from a specific range of the shaft rotation angle α_R. It can be seen from Fig. 22 that the values of $q_{gi(M)}$ should be calculated for angles of rotation α_R of the shaft from any interval $\frac{360^o}{n_{vc}}$. The characteristics of the instantaneous torque working volume $q_{gi(M)}$ and the average value $q_{g(M)}$ are shown in Fig. 23.

The analyses show that the torque working volume of the tested satellite mechanism is $q_{g(M)} = 18.81$ cm^3/rev.

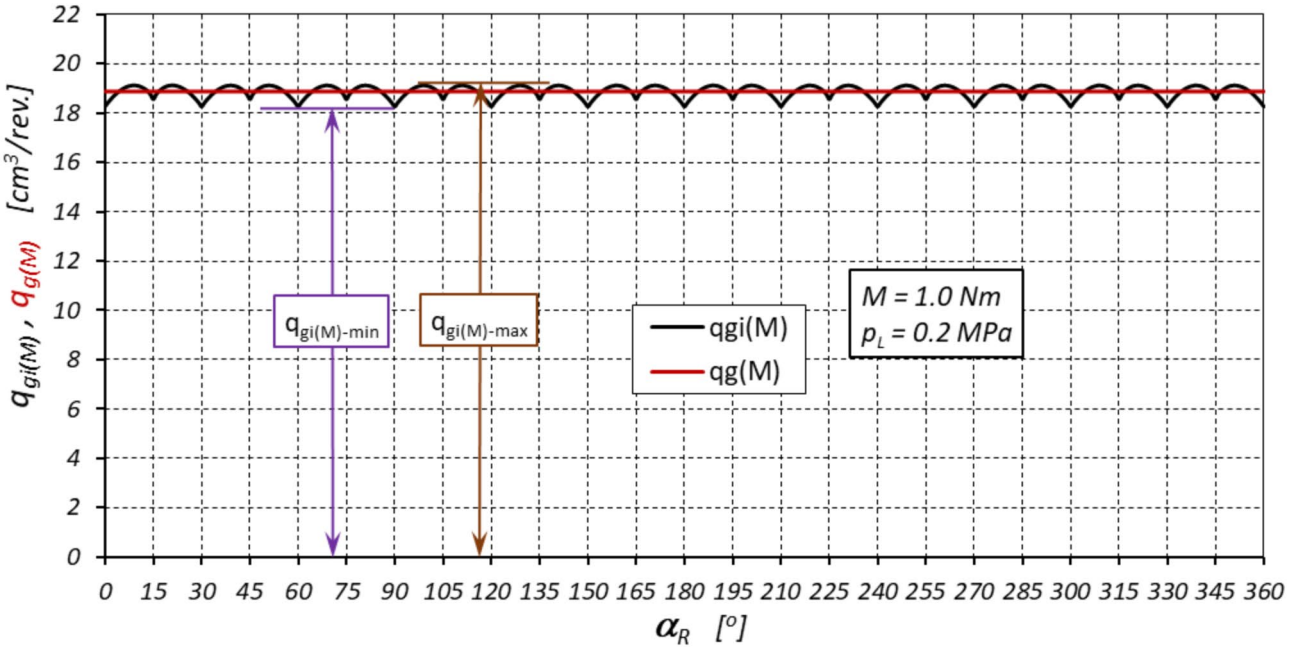

Fig. 23. Characteristics of the instantaneous torque working volume $q_{gi(M)}$ and the average torque working volume $q_{g(M)}$ as a function of the angle of rotation α_R of the rotor (within one complete rotation of the rotor – $\alpha_R = 360°$).

Pressure in the working chambers of the hydraulic motor and the irregularity (pulsation) of the pressure

In a hydraulic motor, the torque M is the load acting on this motor and is therefore a motor-independent parameter[43,44,49]. On the other hand, the pressure p_H in the high-pressure working chamber HPC is the effect of the load M of this motor and also depends on:

1. the geometric working volume q_g;
2. the pressure p_L in the low-pressure working chamber LPC. This pressure is the effect of the pressure drop on the way from the LPC chamber to the liquid reservoir.

Assuming that there are no energy losses in the motor the pressure in the HPC chamber after the transformation of Eq. (39) is therefore:

$$p_H = 2 \cdot \pi \cdot \frac{M}{q_g} + p_L \tag{54}$$

If M = const., q_g = const. and p_L = const. then also p_H = const. and it is an average value.

If, for a hydraulic motor, M = const. (a motor-independent parameter, as mentioned above), the pressure p_H in the HPC chamber changes as a result of the change in the geometric working volume (as a function of the angle of rotation α_R of the shaft). In the HPC chamber of the motor there is therefore an instantaneous pressure p_{Hi}, viz.:

$$p_{Hi} = 2 \cdot \pi \cdot \frac{M}{q_{gi(M)}} + p_L \neq const. \tag{55}$$

The characteristics of the instantaneous p_{Hi} and the average p_H pressure in the high-pressure chamber HPC at M = const. and p_L = const. are shown in Fig. 24.

Since the instantaneous pressure p_{Hi} in the high-pressure chamber HPC is influenced by the instantaneous torque working volume $q_{gi(M)}$, the following applies:

a. the minimum values of the instantaneous pressure $p_{Hi\text{-}min}$ occur for $\alpha_R = \frac{180^o}{n_{ER}} \cdot (1 + 2 \cdot k)$, where k = 0,1,2,….
b. the maximum values of the instantaneous pressure $p_{Hi\text{-}max}$ occur for $\alpha_R = k \cdot \frac{360^o}{n_{ER}}$.

On the other hand, the concept of instantaneous pressure p_{Hi} in the high-pressure chamber HPC of a hydraulic motor is associated with the concept of pressure irregularity δ_p (or otherwise pressure pulsation), defined as:

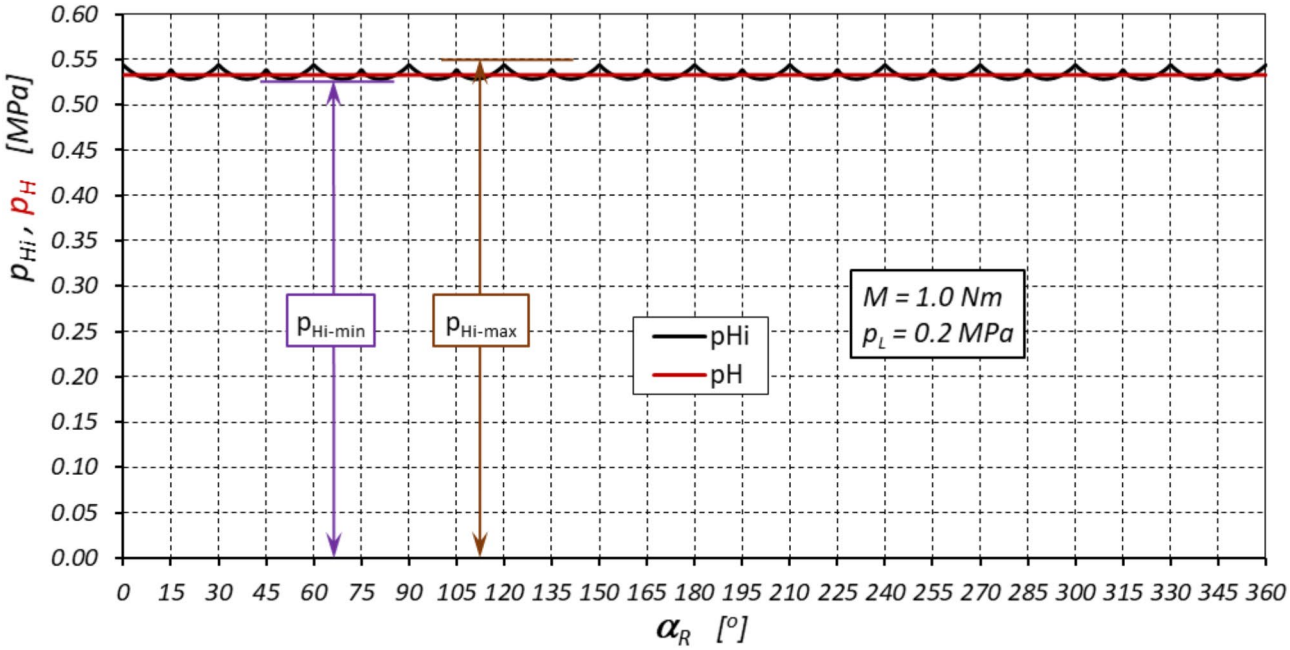

Fig. 24. Characteristics of the instantaneous p_{Hi} and the average pressure p_H as a function of the angle of rotation α_R of the rotor (within one complete rotation of the rotor – $\alpha_R = 360°$).

$$\delta_P = 100 \cdot \frac{p_{Hi-max} - p_{Hi-min}}{p_H} \ [\%] \tag{56}$$

Tested satellite machine

The satellite pump shown in Fig. 25 was the subject of the study. The working mechanism of this pump is shown in Fig. 26. Figure 27 shows the commutation plates as key elements adjacent to the working mechanism. The principle of operating of the satellite pump has been described in detail in the publicly available literature, for example in[42,47,48].

The theoretical working volume of the pump is q_t = 18,87 cm^3/rev.

Test rig

The experimental investigation of the satellite pump was carried out on the test rig shown in Figs. 28 and 29. This stand is equipped with a self-braking worm gear WG (Figs. 28 and 29 (grey)). This gear unit enables the maintance of a constant rotational speed of the shaft of the tested machine TM. The rotation of the shaft of the tested machine TM is possible only when the electric motor E_1 is started. The speed n of the shaft of the tested machine TM can be set by adjusting the rotational speed of the electric motor E_1 using a current frequency converter. The range of the rotational speed n can be set in the range of $n = 0.5 \div 15$ rpm.

The constant pressure drop Δp in the connections of the tested machine TM was maintained by setting the speed of the pump P (and thus its displacement accordingly), the safety valve SV and accumulator A (Fig. 28).

As the displacement machine TM is tested at very low speeds, the flow rate Q_p in this machine will be very small and therefore the pressure drop Δp_{ich} in the internal channels of this machine can be neglected ($\Delta p_{ich} \approx 0$). Then $p_H = p_1$ and $p_L = p_2$.

The measured parameters at the test stand are listed in Table 2.

In the above-mentioned test stand, it is not possible to set and maintain a constant torque on the shaft of the tested machine working as a motor. It is also not possible to test the irregularity of the motor rotational speed at a constant flow rate supplying this motor, as the worm gear maintains a constant speed (n = const.).

The working liquid in the test stand was mineral oil Total Azolla ZS 46.

Results of laboratory tests

The test of the satellite displacement machine was carried out at a low constant speed ($n = 1$ rpm) and two different pressure values p_1 ($p_1 = 5$ MPa and $p_1 = 10$ MPa). For comparison purposes, the tests were carried out for both operation as a pump and operation as a motor. The viscosity of the mineral oil was maintained at a constant level $\nu = 40 \pm 2$ cSt. The following parameters were recorded during the tests:

a. the flow rate Q_p in the machine operating as a pump (Figs. 30) and operating as a motor (Fig. 31) as a function of the angle of rotation α_R of the shaft;

b. the torque M_p on the shaft of the machine operating as a pump (Fig. 32) and operating as a motor (Fig. 33) as a function of the angle of rotation α_R of the shaft.

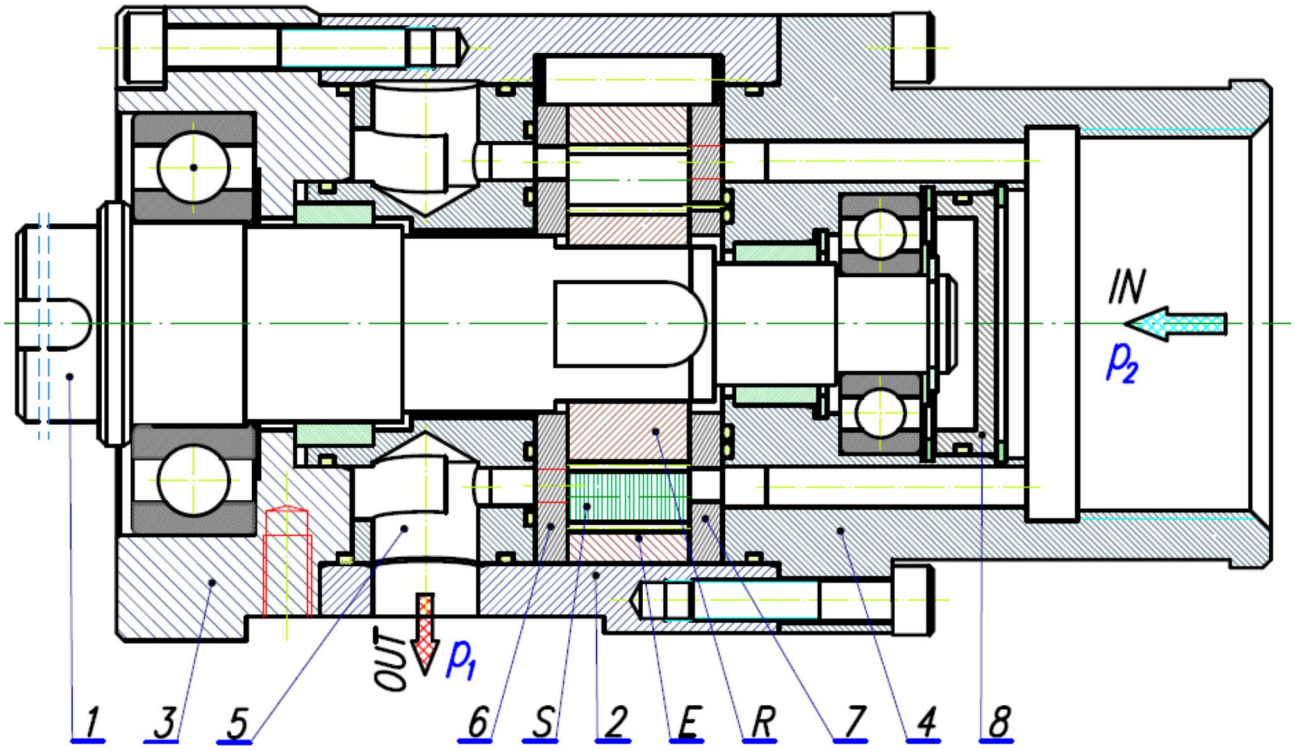

Fig. 25. Tested pump (satellite pump): E – external gear (curvature), S – satellite, R – rotor, 1 – shaft, 2 and 3 – housing, 4 – suction (inflow) manifold, 5 – pumping (outflow) manifold, 6 – high-pressure commutation (compensation) plate, and 7 – low-pressure commutation (compensation) plate, 8 – cover of the shaft chamber.

Discussion

In the satellite working mechanism, the sum of the volumes of all working chambers is constant and independent of the angle of rotation α_R of the shaft (formula (17)). In the satellite mechanism presented in this article, the volume of all working chambers is $V = 13.045\ cm^3$.

In the satellite mechanism, the number of filled chambers at the same time is equal to either the number of humps on the rotor or the number of humps on the curvature. In the considered mechanism type 4×6:

a. if four chambers are filled then:

- six chambers are emptied,
- or four chambers are emptied and the other two chambers are dead (i.e. with maximum or minimum volume);

b. if six chambers are filled, then four chambers are always emptied.

The analysis proves that in the satellite mechanism during the rotation of the rotor (shaft), the value of the working volume changes from the minimum value q_{i-min} to the maximum value q_{i-max} (according to formula (29)).

For a satellite mechanism operating as a pump, the rotational speed of the shaft of the pump is constant ($Q = const.$). Therefore, because of the instantaneous geometric working volume q_{gi}, the displacement Q of the pump will change from the minimum value Q_{i-min} to the maximum value Q_{i-max} as a function of the angle of rotation α_R of the shaft. This means there is an instantaneous delivery Q_i of the pump (formulae (26) and (27)). The number of cycles of change of these values is equal to the number of cycles n_{vc} of change of the volume of all working chambers (formula (11)). The relative change in the value of the delivery was called the pulsation of the delivery δ_Q (formula (33)). The value of this pulsation is the theoretical value and represents the maximum value for the pump.

If the flow rate is constant ($Q = const.$) in the satellite mechanism operating as a motor then due to the existence of the instantaneous geometric working volume q_{gi}, the change in the rotational speed of the shaft will occur (as a function of angle of rotation α_R of the shaft). That is, will be the instantaneous rotational speed n_i of the motor shaft (formula (34)), the value of which changes from n_{i-min} to n_{i-max}. The relative change in the value of this speed was called the pulsation of the rotational speed δ_n (formula (37)). The value of this pulsation is the theoretical value and represents the maximum value for the hydraulic motor.

The results of the analysis show, that in the satellite mechanism:

Fig. 26. Satellite mechanism of the tested satellite pump[15,43,44].

1. the value of pulsation of the rotational speed δ_n (formula (37))is greater than the value of pulsation of the displacement δ_Q (formula(33)). For the satellite mechanism presented in this paper is $\delta_Q = 4.95\%$ and $\delta_n = 5.04\%$;
2. the value of pulsation of the torque δ_M (formula (51)) is greater than the value of pulsation of the pressure δ_p (formula (56)). For the satellite mechanism presented in this paper is $\delta_M = 4.56\%$ and $\delta_n = 3.1\%$.

In the real positive displacement machines (pump and motor) the pressure difference in the working mechanism has an influence on the real values of pulsations. The most important influencing factors are the compressibility of the liquid and leakages in the gaps of the working mechanism. The leakages in the satellite pump and in the motor are described in detail in[47] and[46] respectively.

To summarise, it can be concluded that:

- on the pulsation of the delivery of the pump δ_Q,
- on the pulsation of the torque on the pump shaft δ_M,
- on the pulsation of the pressure in the motor inflow port δ_p,
- on the pulsation of the rotational speed of the motor shaf δ_n.

Fig. 27. Commutation plates: high-pressure commutation plate (left) – position 6 in Fig. 25, low-pressure commutation plate (rightt) – position 7 in Fig. 25.

influences the following parameters:

- the number of the humps n_R of the rotor,
- the number of the humps n_E of the curvature,
- the minimum $A_{ch\text{-}min}$ and maximum $A_{ch\text{-}max}$ values of the working chamber area,
- the height H of the satellite mechanism.

In the satellite mechanism, all pulsations (δ_Q, δ_n, δ_M, δ_p) will decrease when the number of the working chambers, i.e. the number n_E of curvature humps and the number n_R of rotor humps increases. For the satellite mechanisms presented in the publication[15], the lowest pulsation occurs for the mechanism type 8×10 (n_R=8, n_E=10).

Equation (41)÷(50) show that the instantaneous value of the torque $M_{w(ich)}$ „generated" by the one working chamber does not depend on the volume of this chamber, but on the shape of the pitch line of the rotor (i.e. the rotor outline). In each working chamber, the torque from the one satellite is added to the torque from the rotor, but the torque from the second satellite is subtracted (Figs. 18 and 19). This means that the second satellite „lowers" the value of the torque "generated" by the working chamber.

The working volume of the satellite mechanism calculated according to formulae (52) and (53), i.e. based on the torque generated by the working mechanism at certain constant pressures p_H and p_L in the working chambers, is proposed to call the torque working chamber $q_{g(M)}$. The analyses show that the average value of the torque working volume of the considered satellite mechanism is equal to the geometric working volume (i.e. $q_{g(M)} = q_g$) (Fig. 34). This proves that the theoretical analyses were performed out correctly.

The results of the experiment confirmed the results of the theoretical analyses regarding the torque on the pump shaft, i.e. the value of the torque on the pump shaft:

a. is a function of the angle of rotation α_R of the shaft;
b. reaches a minimum every 15° and also a maximum every 15° (Figs. 22 and 31).

If the value of the torque M changes during the rotation of the shaft at a constant rotational speed (n = const.) and at a constant inflow pressure (p_1 = const.), this indicates a change in the value of the volume of the working chamber during this rotation. This in turn confirms the results of theoretical analyses (Figs. 15 and 23). Therefore, if $q_g = f(\alpha_R)$ then also for n = const. is $Q = f(\alpha_R)$ (Fig. 14). The results of the experiment (Figs. 30 and 32) do not show this clearly because the actual flow rate in the positive displacement machine is:

$$Q_p = \underbrace{q_g \cdot n}_{Q} \pm Q_L \tag{57}$$

where Q_L is the volumetric loss (leakage), the sign "+" refers to the hydraulic motor, and the sign "–" refers to the pump. The volumetric losses Q_L are mainly leakages in the timing gaps (leakages in the commutation unit) and

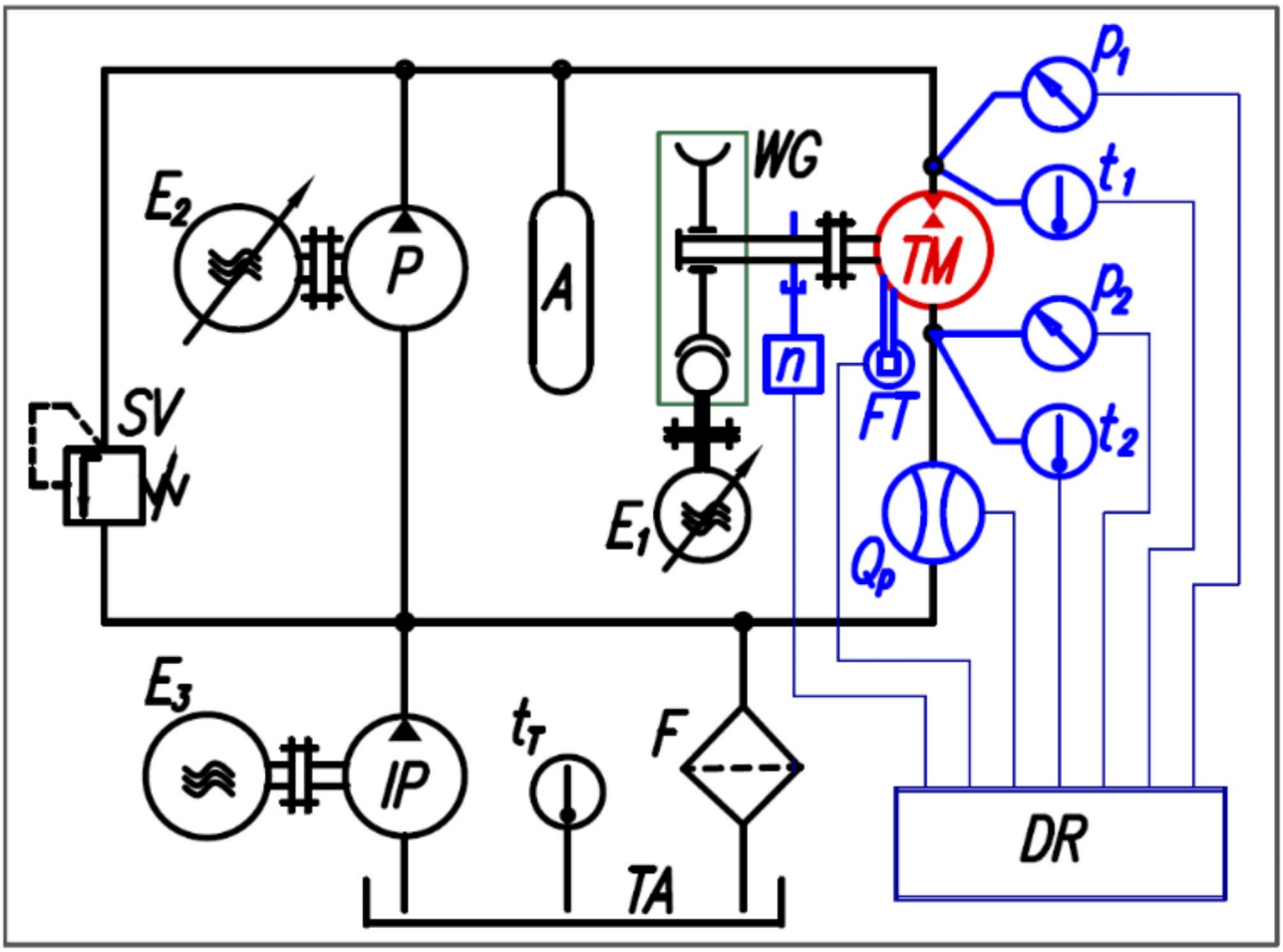

Fig. 28. The test stand – hydraulic system and measuring system: P – pump, TM – tested machine (pump or motor), IP – impeller pump (centrifugal pump), SV – safety valve, F – filter, TA – tank, WG – self-locking worm gear, E_1 and E_2 – electric motors with frequency converters, E_3 – electric motor, DR – data recorder, p_1, p_2 – pressure transducers, t_1, t_2, t_T – temperature transducers, Q_p – flowmeter, FT – force transducer for torque M measurement, n – inductive sensor for rotational speed measurement. (created in Autodesk Autocad 2024, https://www.autodesk.com/)

in the flat gaps of the satellite mechanism. At a very low rotational speed of the shaft, the proportion of this loss Q_L is quite large, especially the loss resulting from leakages in timing gaps (Figs. 30 and 32). The process of these leakages has been described in detail in[35] and leakages in flat gaps in[47,46].

Theoretical analyses show that for $p_1 = 5$ MPa is M = 14.7 Nm and for $p_1 = 10$ MPa is M = 29.4 Nm (Fig. 22). However, the experimental results showed, that the average value of the torque on the shaft of the machine:

1. operating as a pump is greater than the theoretical value of the torque M and is M_p = 23,7 Nm for $p_1 = 5$ MPa and M_p = 42,6 Nm for $p_1 = 10$ MPa (Fig. 31).
2. operating as a hydraulic motor is lower than the theoretical value of the torque M and is M_p = 8.7 Nm for $p_1 = 5$ MPa and M_p = 22.4 Nm for $p_1 = 10$ MPa (Fig. 33).

The relationship between the value of the torque M_p resulting from the experiment and the theoretical value of the torque M is as follows:

$$M_p = M \pm M_L \tag{58}$$

where M_L is the loss of the torque, the sign "–" refers to the hydraulic motor, and the sign "+" refers to the pump. The loss of the torque M_L in the satellite pump and the satellite motor has been described in detail in[48,49].

Summary

The mathematical relationships presented in this article make it possible to calculate the basic operating parameters of hydraulic pumps and motors equipped with any type of satellite mechanism. The correctness of the theoretical analyses of flow rate and torque in the satellite mechanism has been confirmed experimentally. It has also been shown that testing both the pump and the motor at constant speed allows not only the determination

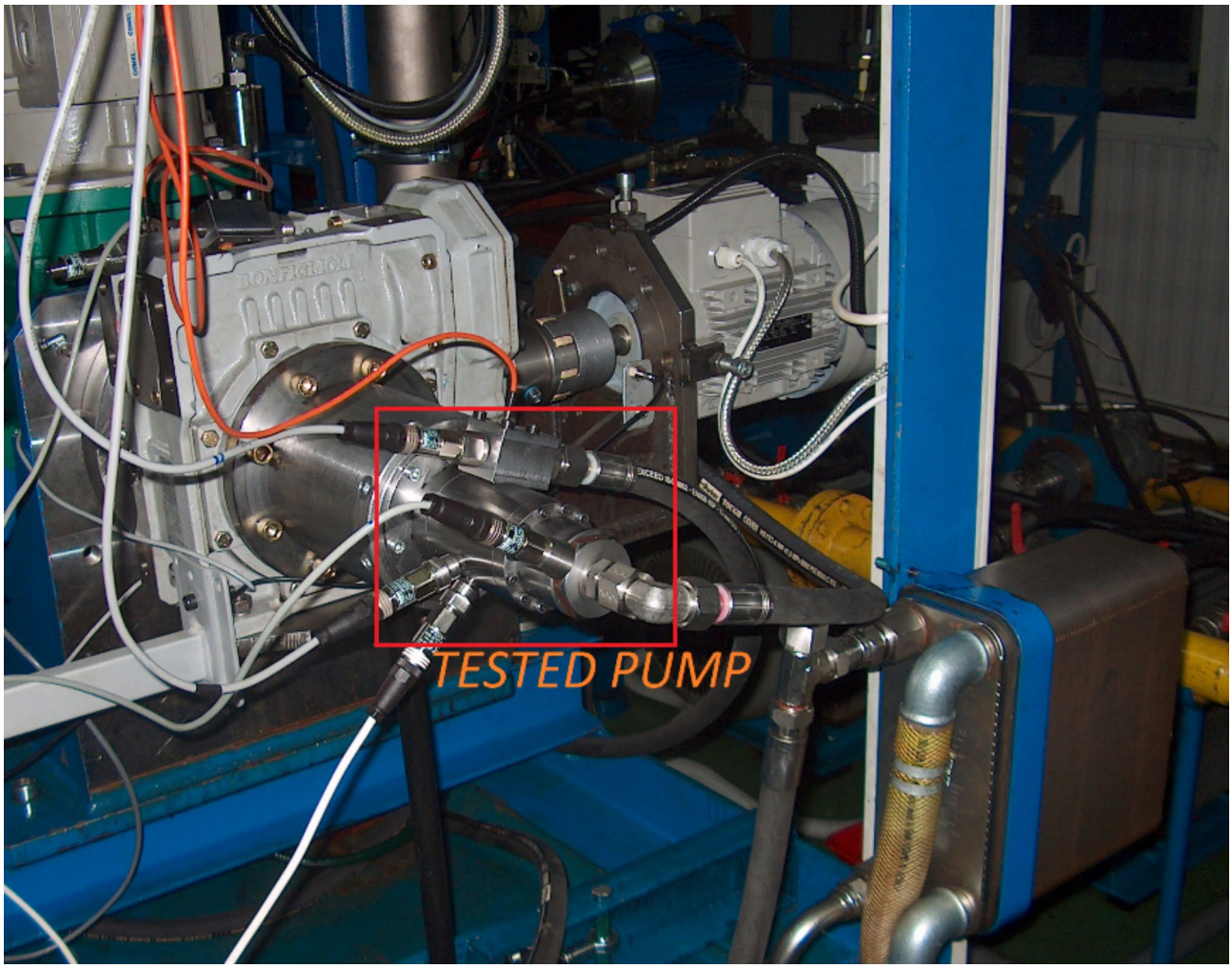

Fig. 29. View of the test stand with worm gear (grey colour) (left) and the satellite pump on the test stand (right).

	Denotatin	Measuring instrument	Range	Class
Pressure	p_1	strain gauge transducer	0 ÷ 25 MPa	0.3
	p_2		0 ÷ 2.5 MPa	0.3
Flow rate	Q	mass flowmeter	0 ÷ 6 l/min	0.1
Torque	FT	strain gauge force transducer	0 ÷ 100 N	0.02
	A	arm fixed to the tested machine body	0.5 m	±0.1 mm
Rotational speed	n	inductive sensor	60.000 rpm	acc. of meas. ±0.01 rpm
Temperature	t_1 and t_2	RTD temperature sensor	180 °C	A

Table 2. Measured parameters and measurements instrument of the test stand (Fig. 28).

of torque and flow rate pulsations but also the observation of the volumetric and mechanical losses that occur in the working mechanism. It can be concluded that low constant speed testing can be considered a fundamental test for prototype hydraulic pumps and motors.

Based on the analyses carried out in this paper, it can be concluded that the satellite mechanisms with the highest number of humps on both the rotor and the curvature will have the best operating characteristics. Therefore, it is advisable to develop and build a displacement machine in the future that contains a satellite mechanism of the 8×10 type. 80 cycles of filling and emptying the working chambers correspond to one full rotation of the rotor of such a mechanism. Such a machine will be therefore characterised by the lowest pressure and speed pulsation (in the case of motor operation) and the lowest capacity and torque pulsation (in the case of pump operation).

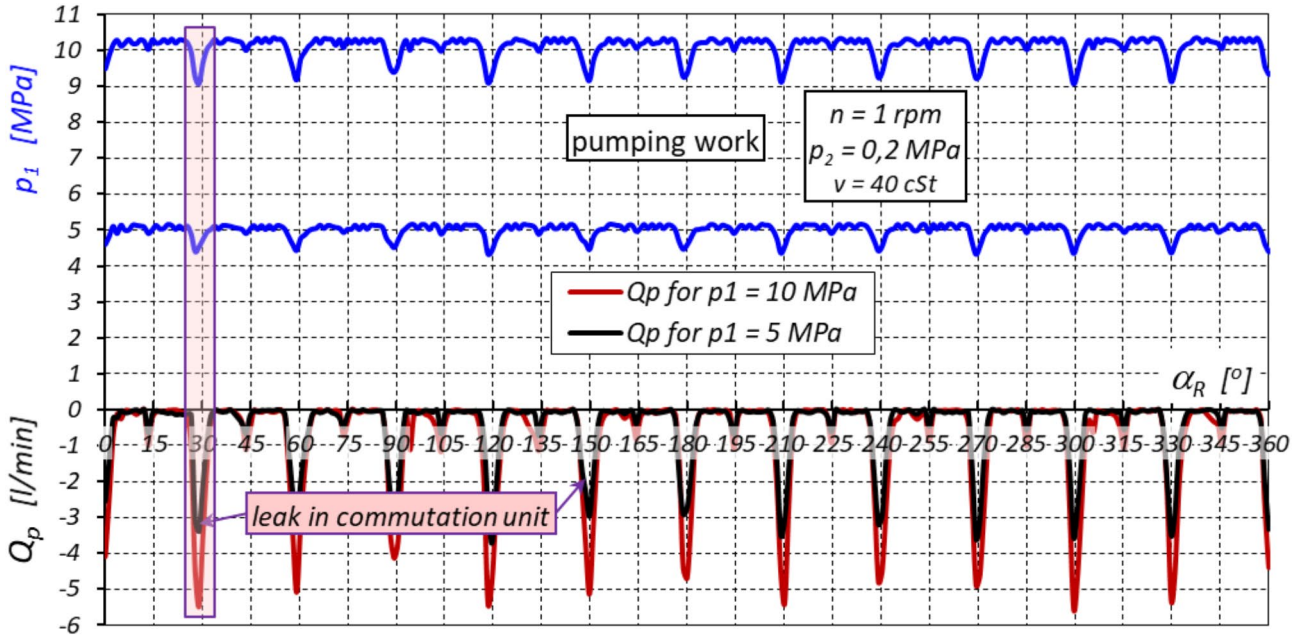

Fig. 30. Characteristics of the actual flow rate Q_p in the machine working as a pump as a function of the angle of rotation α_R of the rotor (within one complete rotation of the rotor – $\alpha_R = 360°$). The pressure loading the pump: $p_1 = 5$ MPa and $p_1 = 10$ MPa.

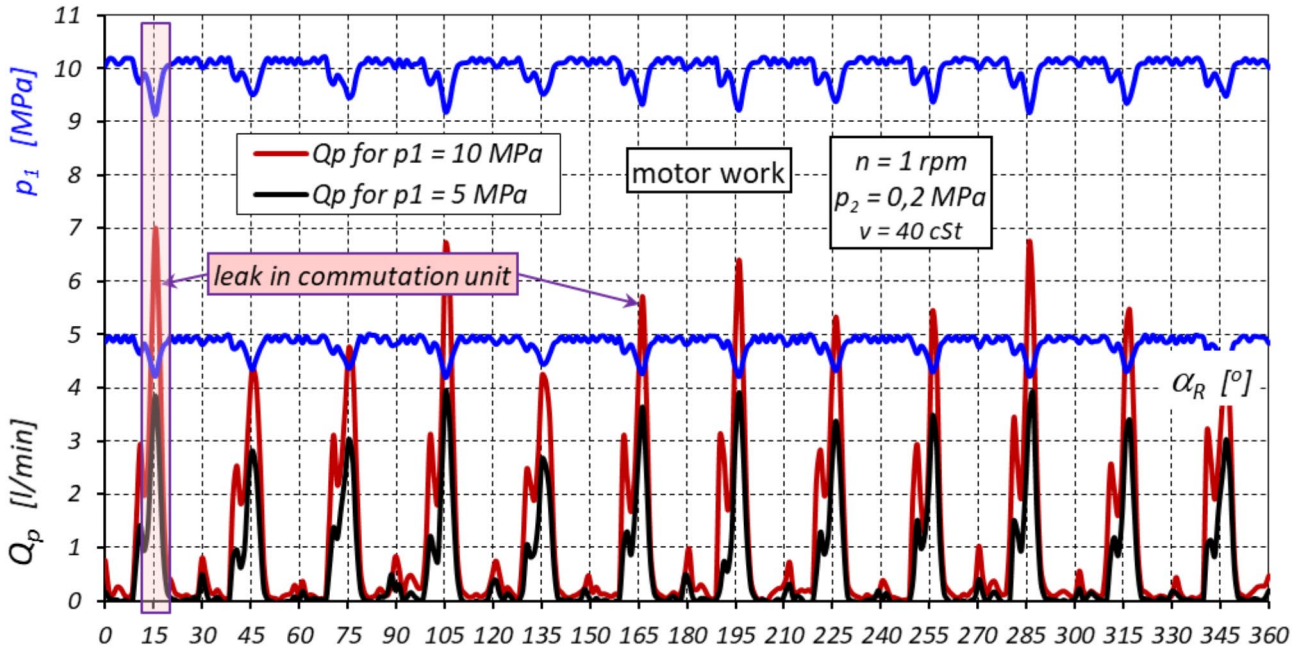

Fig. 31. Characteristics of the actual flow rate Q_p in the machine working as a motor as a function of the angle of rotation α_R of the rotor (within one complete rotation of the rotor – $\alpha_R = 360°$). The pressure in the inflow port of the motor: $p_1 = 5$ MPa and $p_1 = 10$ MPa.

The theoretical analyses presented in this paper form the starting point for the development of a mathematical model of rotational speed and pressures in a multi-speed satellite motor, i.e. the so-called digital satellite motor.

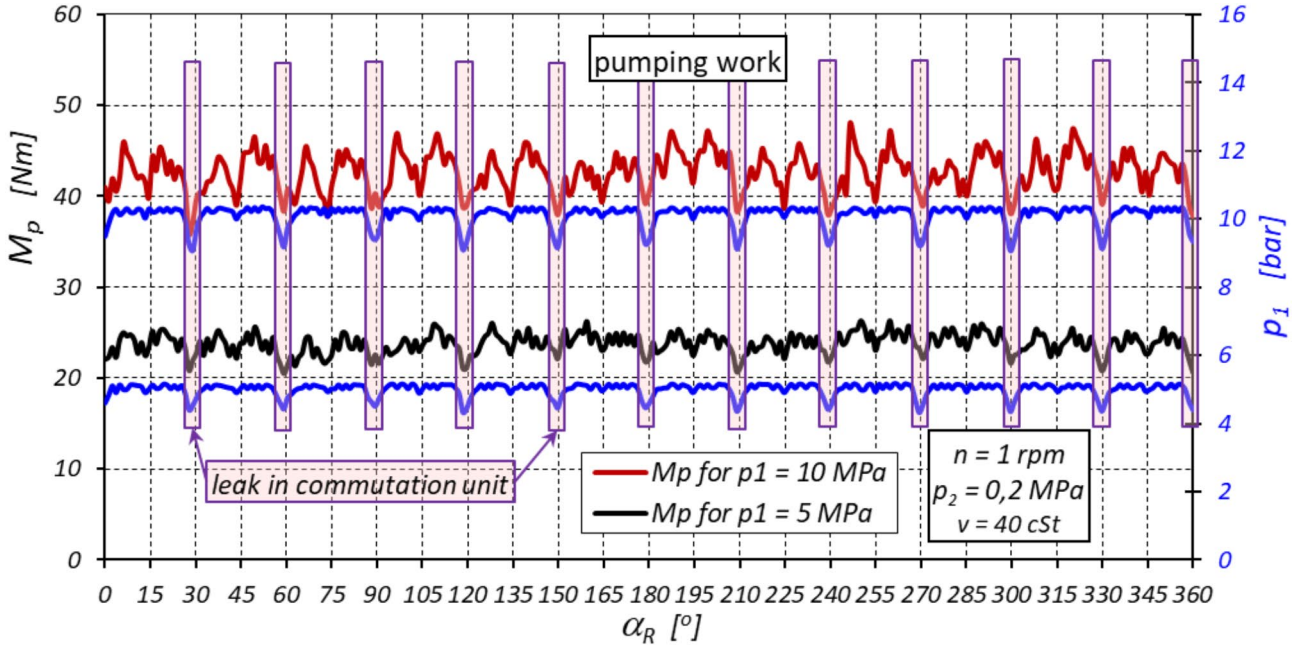

Fig. 32. Characteristics of the torque M_p on the shaft of the machine working as a pump as a function of the angle of rotation α_R of the rotor (within one complete rotation of the rotor – $\alpha_R = 360°$). The pressure loading the pump: $p_1 = 5$ MPa and $p_1 = 10$ MPa.

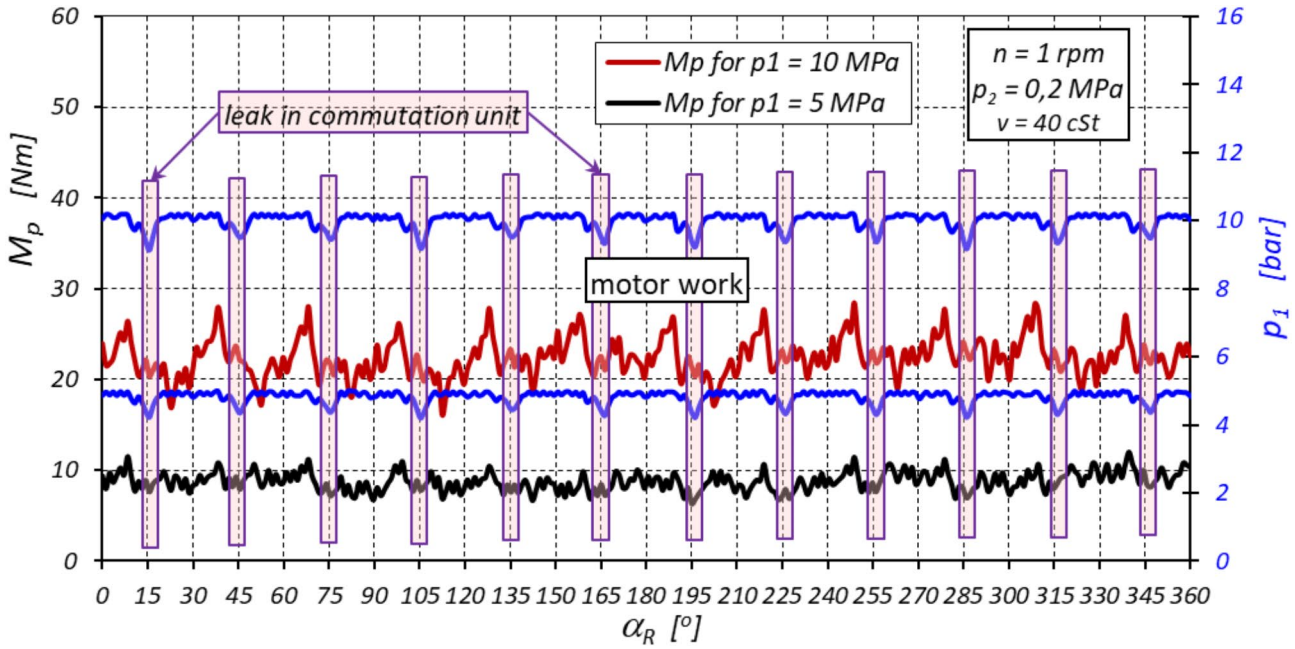

Fig. 33. Characteristics of the torque M_p on the shaft of the machine working as a motor as a function of the angle of rotation α_R of the rotor (within one complete rotation of the rotor – $\alpha_R = 360°$). The pressure in the inflow port of the motor: $p_1 = 5$ MPa and $p_1 = 10$ MPa.

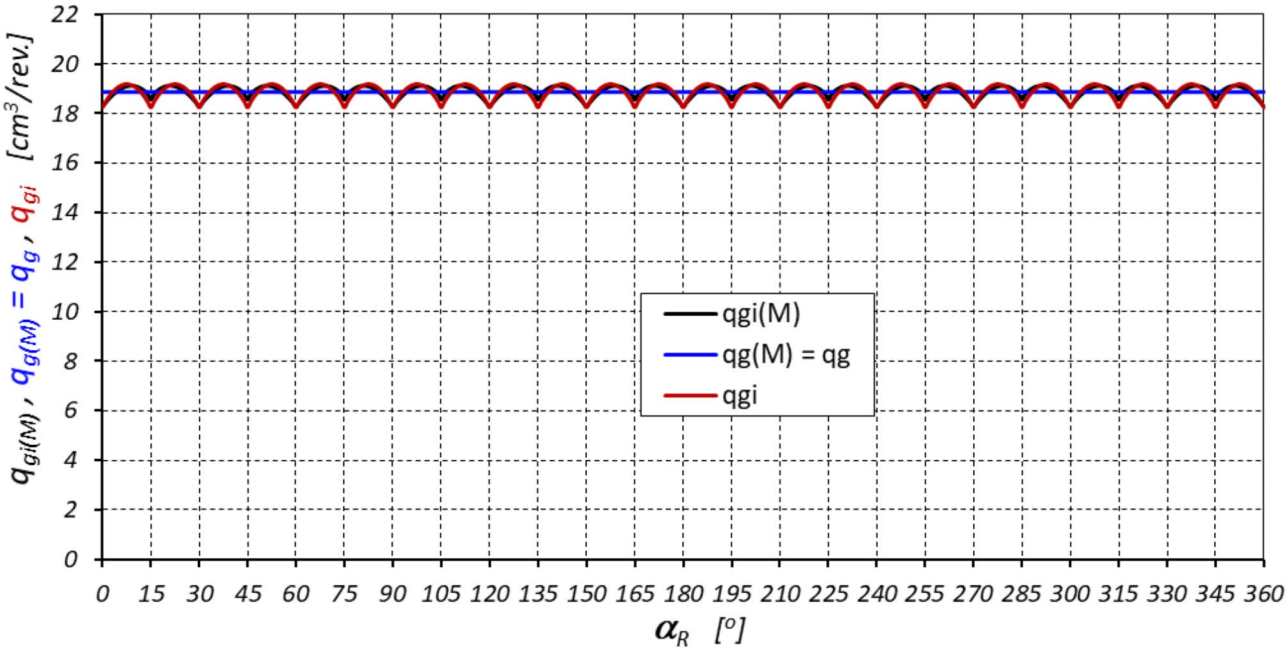

Fig. 34. Comparison of the instantaneous and average torque working volume ($q_{gi(M)}$ and $q_{g(M)}$) with the instantaneous and average geometric vorking volume (q_{gi} and q_g) calculated according to formulae (29) and (30).

Data availability

The datasets used and/or analysed during the current study are available from the corresponding author on reasonable request.

Received: 6 November 2024; Accepted: 1 April 2025
Published online: 12 April 2025

References

1. Sieniawski, B. Silnik Hydrauliczny obiegowo-krzywkowy (eng. Rotary-cam hydraulic motor). Patent PL 71329. https://ewyszukiwarka.pue.uprp.gov.pl/search/pwp-details/P.151883?lng=pl (1974).
2. Balawender, A. *Analiza energetyczna i Metodyka Badań Silników Hydraulicznych Wolnoobrotowych* (*Energy analysis and methodics of testing of low-speed hydraulic motors*). (Scientific Book of the Gdansk University of Technology, Mechanika No. 54. Gdansk University of Technology Publishing House, 1988).
3. Ulatowska, A. Parametric 3D model of a planetary gear motor. *Czas Tech. Mech.* 105. https://repozytorium.biblos.pk.edu.pl/resources/33942 (2008).
4. Stryczek, S. *Napęd Hydrostatyczny* (WNT, 2005).
5. JianGang, L., XuTang, W. & ShiMin, M. Numerical computing method of noncircular gear tooth profiles generated by shaper cutters. *Int. J. Adv. Man. Tech.* https://doi.org/10.1007/s00170-006-0560-0 (2007).
6. Jasinski, R. Analysis of the heating process of hydraulic motors during start-up in thermal shock conditions. *Energies* https://doi.org/10.3390/en15010055 (2022).
7. Catalog of of satellite motors type SOK of Hydro-precyzja company. https://www.hydro-precyzja.pl/ (Access date 10 Oct 2024).
8. Kujawski, M. *Mechanizmy Obiegowe Z Nieokrągłymi Kołami Zębatymi, Podstawy Projektowania I Wykonania (eng. Circulation Mechanisms with non-circular Gears: the Basics of Design and manufacturing)* (Poznan University of Technology Publishing House, 1992).
9. Catalog of satellite motors of SM-Hydro company. https://smhydro.com.pl (Access date 10 Oct 2024).
10. Catalog of satellite motors of PONAR company. https://www.ponar-wadowice.pl/en/n/new-product-satellite-motors (Access date 10 Oct 2024).
11. Catalog of satellite motors of HYDROMECH company. https://hydromechsa.pl/pl/produkcja/planetarne-silniki-hydrauliczne-emulsyjne-i-olejowe (Access date 10 Oct 2024).
12. Sieniawski, B. & Potulski, H. Hydrauliczny Silnik satelitowy (eng. Hydraulic satellite motor). *Patent PL* 137642. https://ewyszukiwarka.pue.uprp.gov.pl/search/pwp-details/P.234335?lng=pl (1984).
13. Sieniawski, B. Maszyna Wyporowa typu obiegowo-krzywkowego Z Kompensacją Luzów, Zwłaszcza Jako Silnik Hydrauliczny O Dużej Chłonności (eng. Planetary cam type displacement machine with axial play taking up feature, in particular that used as a hydraulic motor of high specific absorbing capacity). *Patent PL* 185724. https://ewyszukiwarka.pue.uprp.gov.pl/search/pwp-details/P.321438?lng=pl (1997).
14. Balawender, A., Elgert, K., Gumos, M., Sobiechowski, T. & Sliwinski, P. Directions of research work on hydraulic satellite motors with axial clearance compensation. *Hyd I Pneum* 4. https://www.researchgate.net/publication/382130564_Directions_of_research_work_on_hydraulic_satellite_motors_with_axial_clearance_compensation#fullTextFileContent (2003).
15. Sliwinski, P. The methodology of design of satellite working mechanism of positive displacement machine. *Sci. Rep.* **12**, 13685. https://doi.org/10.1038/s41598-022-18093-z (2022).
16. Volkov, G. & Kurasov, D. Planetary rotor hydraulic machine with two central gearwheels having similar tooth number. In *Advanced Gear Engineering. Mechanisms and Machine Science* vol. 51. https://doi.org/10.1007/978-3-319-60399-5_21 (Springer, 2018).

17. Kurasov, D. Geometric calculation of planetary rotor hydraulic machines. *IOP Conf. Ser. Mat. Sci. Eng.* https://doi.org/10.1088/1757-899X/862/3/032108 (2020).
18. Volkov, G., Fadyushin, D. & Vedernikov, M. Geometric calculation of non-circular gear segments of the planetary mechanism in rotary hydraulic machines. *E3S Web of Conf.* https://doi.org/10.1051/e3sconf/202338901017 (2023).
19. Volkov, G., Kurasov, D. & Gorbunov, M. Geometric synthesis of the planetary mechanism for a rotary hydraulic machine. *Russ Eng. Res.* https://doi.org/10.3103/S1068798X18010161 (2018).
20. Volkov, G. & Fadyushin, D. Improvement of the method of geometric design of gear segments of a planetary rotary hydraulic machine. *JOP Conf. Ser. J. Phys.* https://doi.org/10.1088/1742-6596/1889/4/042052 (2021).
21. Wang, C., Luan, Z. H. & Gao, W. P. Design of pitch curve of internal-curved planet gear pump strain in type N-G-W based on three-order ellipse. *AMR*. https://doi.org/10.4028/www.scientific.net/amr.787.567 (2013).
22. Kurasov, D. Selecting the shape of centroids of round and non-round gears. *IOP Conf. Ser. Mat. Sci. Eng.* https://doi.org/10.1088/1757-899X/919/3/032028 (2020).
23. Volkov, G., Smirnov, V. & Mirchuk, M. Estimation and ways of mechanical efficiency upgrading of planetary rotary hydraulic machines. *IOP Conf. Ser. Mat. Sci. Eng.* https://doi.org/10.1088/1757-899X/709/2/022055 (2020).
24. Liu, Y., Wu, L., Dong, C. & Wang, F. Investigation of contact ratio and dynamic characteristics of non-circular planetary gear train in hydraulic motor. *Flow. Meas. Inst.* **100**, 102720. https://doi.org/10.1016/j.flowmeasinst.2024.102720 (2024).
25. Li, D., Liu, Y., Gong, J. & Wang, T. Design of a noncircular planetary gear mechanism for hydraulic motor. *Mat. Prob Eng.* **2021**, 5510521. https://doi.org/10.1155/2021/5510521 (2021).
26. Zhang, B., Song, S., Jing, C. & Xiang, D. Displacement prediction and optimization of a non-circular planetary gear hydraulic motor. *Adv. Mech. Eng.* https://doi.org/10.1177/16878140211062690 (2021).
27. Wang, K., Gao, Z., Chen, G. & Guo, M. Tooth profile construction and experimental verification of non-circular gear based on double Arc active design. *Appl. Sci.* **13**, 10566. https://doi.org/10.3390/app131910566 (2023).
28. Sliwinski, P. Mechanizm satelitowy Hydraulicznej Maszyny Wyporowej (Satellite operating mechanism of a hydraulic displacement machine). Patent application P.445213. https://ewyszukiwarka.pue.uprp.gov.pl/search/pwp-details/P.445213 (2023).
29. Oshima, S. & Hiranao, T. Investigation for output torque of a low pressure water hydraulic planetary gear motor. *Ventil* **18**(1), http://www.dlib.si/?URN=URN:NBN:SI:doc-0500MONK (2012).
30. Oshima, S., Hirano, T., Miyakawa, S. & Ohbayashi, Y. Study on the output torque of a water hydraulic planetary gear motor. In *Proceeding of The Twelfth Scandinavian International Conference on Fluid Power SICFP'11, Tampere, Finland*. https://trepo.tuni.fi//handle/10024/116713 (2011).
31. Oshima, S., Hirano, T., Miyakawa, S. & Ohbayashi, Y. Development of a rotary type water hydraulic pressure intensifier. *Int. J. Fluid Power Sys*. https://doi.org/10.5739/jfpsij.2.21 (2009).
32. Liu, Y., Ren, X. & Dong, C. Transmission performance analysis of non-circular gear hydraulic motor. *Jor J. Mech. Ind. Eng.* https://doi.org/10.59038/jjmie/180316 (2024).
33. Sliwinski, P. Determination of the theoretical and actual working volume of a hydraulic motor – Part II (The method based on the characteristics of effective absorbency of the motor). *Energies* **14**(6), 1648. https://doi.org/10.3390/en14061648 (2021).
34. Sliwinski, P. Geometric working volume of a satellite positive displacement machine. *Sci. Rep.* **14**, 11195. https://doi.org/10.1038/s41598-024-61773-1 (2024).
35. Sliwinski, P. The basics of design and experimental tests of the commutation unit of a hydraulic satellite motor. *Arch. Civ. Mech. Eng.* https://doi.org/10.1016/j.acme.2016.04.003 (2016).
36. Smirnov, V. & Volkov, G. Computation and structural methods to expand feed channels in planetary hydraulic machines. *IOP Conf. Series: J. Phys.* https://doi.org/10.1088/1742-6596/1210/1/012131 (2019).
37. Sieniawski, D. *Pompa obiegowa (Circulating pump)*. Master thesis. (Gdansk University of Technology, 1984).
38. Ding, H. Application of non-circular planetary gear mechanism in the gear pump. *Adv. Mat. Res.* https://doi.org/10.4028/www.scientific.net/AMR.591-593.2139 (2012).
39. Luan, Z. & Ding, M. Research on non-circular planetary gear pump. *Adv. Mat. Res.* https://doi.org/10.4028/www.scientific.net/AMR.339.140 (2011).
40. Osiecki, L. Rozwój konstrukcji pomp satelitowych (eng. *Development of satellite pump structures*). *Nap. i Ster.* **12**. http://nis.com.pl/userfiles/editor/nauka/122018_n/Osiecki.pdf (2018).
41. Osiecki, L. New generation of the satellite hydraulic pumps. *J. Mech. Energy Eng.* https://doi.org/10.30464/jmee.2019.3.4.309 (2019).
42. Sliwinski, P. Pompa satelitowa (Satellite pump). Patent PL 244928. https://ewyszukiwarka.pue.uprp.gov.pl/search/pwp-details/P.439702 (2024).
43. Sliwinski, P. Influence of geometrical and operational parameters on tooth wear in the working mechanism of a satellite motor. *Sci. Rep.* **13**, 17028 (2023). https://www.nature.com/articles/s41598-023-44319-9
44. Sliwinski, P. Influence of operating pressure on the durability of a satellite hydraulic motor supplied by rapeseed oil. *Sci. Rep.* **14**, 10441. https://doi.org/10.1038/s41598-024-61072-9 (2024).
45. Cao, W., Liu, Y., Niu, Z. & Wang, L. Leakage characteristics analysis of an end face clearance compensated non-circular planetary gear motor. In *IEEE 8th International Conference on Fluid Power and Mechatronics (FPM), Wuhan, China*. https://ieeexplore.ieee.org/document/9035879/metrics#metrics https://doi.org/10.1109/FPM45753.2019.9035879 (2019).
46. Sliwinski, P. The influence of water and mineral oil on volumetric losses in a hydraulic motor. *Pol. Mar. Res*. https://doi.org/10.1515/pomr-2017-0041 (2017).
47. Sliwinski, P. The influence of water and mineral oil on volumetric losses in the displacement pump for offshore and marine applications. *Pol. Mar. Res.* https://doi.org/10.2478/pomr-2019-0037 (2019).
48. Sliwinski, P. The influence of water and mineral oil on mechanical losses in the displacement pump for offshore and marine applications. *Pol. Mar. Res.* https://doi.org/10.2478/pomr-2018-0040 (2018).
49. Sliwinski, P. The influence of water and mineral oil on mechanical losses in a hydraulic motor for offshore and marine applications. *Pol. Mar. Res.* https://doi.org/10.2478/pomr-2020-0034 (2020).
50. Sliwinski, P. & Patrosz, P. Methods of determining pressure drop in internal channels of a hydraulic motor. *Energies*. https://doi.org/10.3390/en14185669 (2021).
51. Kujawski, M. Pulsacja Chłonności i Momentu Obrotowego Obiegowych Silników Hydraulicznych. *Maszyny Górnicze* **3**(53). (1995).
52. Kujawski, M. Ustalenie Ogólnych Równań i Algorytmu Ich Rozwiązywania W Celu Wyznaczenia Chłonności Właściwej Obiegowych Silników Hydraulicznych (eng. Determine the general equations and their solution algorithm for determining the specific absorption of Circulating hydraulic motors). *Maszyny Górnicze* **70** (1997).
53. Kujawski, M. Metody Wyznaczania Głównych parametrów Eksploatacyjnych Obiegowych Silników Hydraulicznych Z Nieokrągłymi Kołami zębatymi (eng. Methods for determining the main operating parameters of Circulating hydraulic motors with non-circular gears). *Hyd Pneum* **1** (1996).
54. Drogosz, P. Teoretyczne badanie chłonności obiegowych silników hydraulicznych (eng. Theoretical study of the absorption of circulating hydraulic motors.). Ph.D. dissertation. (Poznan University of Technology, 2001).
55. Kujawski, M. Analiza kinetostatyczna Obiegowych Silników Hydraulicznych Z Nieokrągłymi Kołami zębatymi. *Maszyny Górnicze* **5**(59) (1996).

Author contributions
The manuscript was written entirely by the author.

Declarations

Competing interests
The authors declare no competing interests.

Additional information
Correspondence and requests for materials should be addressed to P.S.

Reprints and permissions information is available at www.nature.com/reprints.

Publisher's note Springer Nature remains neutral with regard to jurisdictional claims in published maps and institutional affiliations.